Department of Primary Industries
Department of Regional NSW

Climate Change Research Strategy

NSW Drought in a Changing Climate

Technical Report

NSW GOVERNMENT

Authors

Anthony Clark, Jennifer Wurtzel, Esther Zhu, Kim Broadfoot.

Funding

Proudly funded by the NSW Government. This work has been completed as part of the NSW Primary Industries Climate Change Research Strategy funded by the NSW Climate Change Fund.

Suggested Citation

NSW Department of Primary Industries (2024). *NSW Drought in a Changing Climate Technical Report*, Climate Change Research Strategy. NSW Department of Primary Industries.

Acknowledgement of Country

The Department of Primary Industries acknowledges that it stands on Country which always was and always will be Aboriginal land. We acknowledge the Traditional Custodians of the land and waters, and we show our respect for Elders past, present and emerging. We are committed to providing places in which Aboriginal people are included socially, culturally and economically through thoughtful and collaborative approaches to our work.

Copyright Statement

Abbreviations

AET	Actual evapotranspiration
ANUSPLIN	Laplacian thin plate smoothing splines
BC	Blaney-Criddle
CCRS	Climate Change Research Strategy
CDF	Cumulative distribution function
CDI	Combined Drought Indicator
CF	Correction factor
CMIP	Coupled Model Intercomparison Project
EDIS	Enhanced Drought Information System
ESD	Empirical-Statistical Downscaling
FDF	Future Drought Fund
FMD	Farm Management Deposit
GCM	General Circulation Model
GLM	Generalised Linear Model
GPP	Gross Primary Productivity
HS	Hargreaves-Samani
JRA	Gridded reanalysis data set
MDI	Minimum Drought Index
NCI	Australian National Computing infrastructure
NSW	New South Wales
PET	Potential evapotranspiration
PGI	Plant Growth Index
PM	Penman-Monteith
RI	Rainfall Index
RMSE	Root mean squared error
SSR	Singularity Stochastic Removal
SWI	Soil Water Index
VA	Vulnerability Assessment

Contents

List of figures

Executive Summary

Overview of findings

The results of this study concur with the general conclusion of previous scientific evaluations for Australia and globally, that the nature of drought events is likely to change in south-eastern Australia over the 21st century. The most likely shift is towards more prolonged and severe droughts for most of NSW, given the influence of anthropogenic global climate change.

While the overall scenario is for worsening risk of drought across most of the state, this study found there are small areas within NSW, mainly the higher elevations of the tablelands and eastern ranges, where changes appear to be less severe. This finding is unique in the context of previous assessments of drought under climate change for Australia and requires further ratification.

Approach to developing future drought scenarios

This work program was designed to build an updated and high-resolution analysis of drought under climate change for NSW. This involved work to develop and then integrate three main components:

- the acquisition and empirical downscaling of the most recent climate change projection ensemble sourced from the Coupled Model Intercomparison Project 6 (CMIP 6).
- Use of new high resolution climate observation data (ANUClimate) at a 1km^2 resolution.
- the multi-indicator drought monitoring framework used operationally in NSW for the 2017-2019[1] drought event (Enhanced Drought Information System, EDIS).

The resulting future drought scenarios for NSW are expressed as changes in key drought properties (duration and frequency) from a 1995-2014 baseline, the lived experience of most land managers including part of the millennium drought sequence.

Like many assessments of future drought there should be medium confidence placed in the future scenarios generated by this methodology. The main limitations of the approach are described in more detail below along with some insights into future lines of work that may improve confidence.

[1] The entry of the '2017-2019' drought started in late 2016, while the recovery extended into 2020.

Baseline drought risk for NSW

The historical exposure profile, or statistics of historical risk of drought have been rarely published in Australia, so it is important to first consider the baseline scenario to interpret the key findings of this study.

For the 1995-2014 baseline regional NSW spends between 10-20 percent of its time in drought conditions, with the average duration of an event between 200-500 days (1 to 1.5 years). Drought events can extend to up to 1000 days (2-3 years) in duration. The frequency of drought is moderate-to-high in NSW, with regions experiencing 4-8 drought events across a 20-year timeframe. There is spatial variability in baseline drought risk between regions, with parts of the coast and isolated regions along the Great Dividing Range experiencing some of the most variable conditions.

Finding 1: Adverse changes to future drought characteristics across most of NSW

This report's main findings are that even under the low-end greenhouse gas emissions scenario in the medium-term future (2041-60), drought events are likely to be 50-200 days longer, there tend to be 1-3 more events over a 20-year management window, and the time spent in drought increases by 10-20 percent for much of the state.

Under the more severe emissions scenario in the far future (2081-2100), these general downside changes to drought characteristics become more pronounced. Drought durations lengthen considerably by one to two years, they are relatively frequent events in the central to western districts of NSW and the time spent in drought increases by 20-50 percent in most areas.

Finding 2: Limited change to drought characteristics in some NSW regions

The generally adverse scenarios described above do not hold for all regions of the state. Even in the far future (2081-2100) and under the extreme emissions scenario, drought characteristics remain unchanged or may improve slightly in the upper tablelands and Great Dividing Range. This region and some parts of the coastal hinterland appear partially buffered to future shifts in rainfall and temperature, potentially because of their unique topographic position and aspect.

Finding 3: GCM quality assessment is important at a regional level, particularly in Northern NSW

The main findings of the study, the general state-level forward drought projections and scenarios, were not overtly influenced by the main assumptions about methods tested in this study. This included the methodology for determining Potential Evaporation (PET) and whether to account for Global Climate Model (GCM) quality when analysing a model

ensemble. Different PET methods resulted in some minor differences in the forward drought scenarios at local scales within regions, but did not change overall trends and patterns across the state.

Although the main findings at state level were robust, the regional and sub-regional (farm-to-farm) distribution of results were influenced by aspects of the methodology. Accounting for GCM quality did introduced differences at a regional level, particularly to the north of NSW under a higher emissions scenario in the far future. For example, not accounting for GCM quality could lead to an underestimate of change in average drought duration in this part of NSW by 100-200 days when the estimated change signal is in the order of a 200-300 day increase. This is likely due to the well-known inter-model differences across GCM ensembles in estimating the latitudinal position of the South Pacific Convergence Zone that affects seasonal variability in northern Australia. This re-enforces the need to include regional-level methods, like finer scale climate modelling, in this and other ensemble studies in an effort to build more robust future climate change scenarios for planning.

Important limitations and recommendations

The future drought scenarios for NSW described above are far from definitive planning storylines, particularly the identification of positive change in some regions. Analysing drought in a changing climate is complex, and the high-resolution methodology (1km^2 grid across NSW) developed for this study is used with full knowledge of its limitations. As it used predominantly empirical methods and the land and atmosphere are loosely integrated, it does not include some feedbacks like land surface-climate interactions. These types of feedbacks and interactions could change the relationships on which the methodology is built, and either temper or amplify the regional change patterns of drought described in the forward scenarios.

Given this limitation it is important that decision-makers consider them as interim findings and use them as guidance to plan for a wide range of scenarios at this stage, at least until the results are ratified in other studies. Regional to sub-regional change analyses at the scale of this study are rare, and they lack the multiple lines of evidence that underpin the global impact assessments put forward by the IPCC.

Improving the quality of future regional drought assessments by explicitly including feedback is an important undertaking if more definitive planning storylines are required at a farm to regional scale. This includes repeating studies like this one with regional climate models and paleoclimate reconstructions, as well as application of fully coupled land-atmosphere-ocean models.

Introduction

Drought is a major risk for the primary production sector of New South Wales (NSW), bringing significant challenges for farmers, industry and governments. In the most recent event from 2017-2019, south-eastern Australia experienced a widespread and severe drought. While the event had a number of distinct phases, in aggregate, it had the longest duration and widest extent across NSW of any drought in recent recorded history (Figure 1).

The direct impacts on the state were large, and the NSW economy experienced an estimated $20 billion loss in Gross Domestic Product (GDP) over the three years (Wittwer and Waschik 2021). The initial phase of the event was a widespread and unprecedented agronomic drought, with acute fodder shortages and lack of agistment options for livestock producers. Over time the event intensified into a severe meteorological and hydrological drought with associated impacts on water resource availability on farms and in rural communities. At this point the event began to propagate into a range economic, social and ecological impacts. The mild improvement in grass growth conditions and the arrival of unusually warm and dry weather at the end of the drought created conditions for widespread bushfires across NSW, which ran from late winter of 2019 through the 2019-20 summer. For the agricultural sector, one significant cumulative impact was a decline in farm capital across most regions in the state, which remained well after the climatic event receded in early 2020 (Wittwer and Waschik 2021).

Australian Governments commit large amounts of resources to within drought responses and support measures, as well as investing in resilience building in preparation for drought. For instance, the NSW Government committed an estimated $4.5 billion to drought response programs for the 2017-2019 event (Regional NSW, 2022). Over the course of the event farmers in NSW also accessed $200 million from one of the Commonwealth Government's key resilience measures, the national Farm Management Deposit (FMD). This is the first fall in the NSW component of the FMD since its creation in 1999 (DAWE, 2021). In June 2020, the Commonwealth Government created the Future Drought Fund, with a $5 billion commitment at an annual investment target of $ 100 million. An estimated $420 million had been allocated to resilience programs by the end of 2021 (DAWE 2022).

Given these impacts and the levels of financial investment in drought management by governments, there is considerable interest in how the characteristics of drought experienced in NSW could evolve in the medium to long-term future under climate change. To plan for the future, decision-makers in government and industry require information such as anticipated changes in the frequency, duration and intensity of drought events. To develop projected scenarios of drought, this study leverages the

operational framework used by NSW Department of Primary Industries (DPI) to monitor the 2017-2019 drought, known as the NSW Enhanced Drought Information System (EDIS). Scenarios of future drought out to 2100 are produced by running EDIS with an ensemble of the latest Global Circulation Models that were downscaled to a regional to farm level for this purpose.

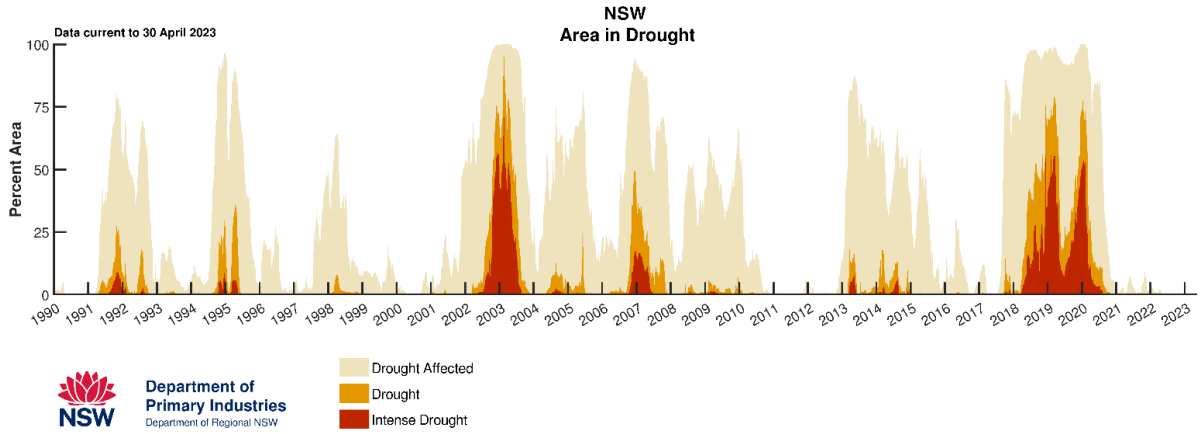

Figure 1. Recent NSW drought history (January 1990- April 2023) as depicted by the NSW-Combined Drought Indicator (CDI), which is part of the NSW DPI Enhanced Drought Information System (EDIS). Data are time series of the percentage area of NSW under drought conditions.

Guide to the technical report

This technical report targets both general and technical audiences. The technical report can be read selectively depending on the interest and objectives of differing stakeholders. The report has been structured with this in mind where:

- all readers are encouraged to review the Methodology section to understand how the drought scenarios were developed.
- the appendices on Empirical-Statistical Downscaling and Evapotranspiration will interest a technical audience seeking more detail about these aspects of the methodology.
- for decision makers, the key section for review is the description of NSW Drought Scenarios, although this will be relevant to all readers.

Background and objectives of this study

This study forms part of the NSW Climate Change Research Strategy for Primary Industries (CCRS). It is part of the Climate Resilience theme of the CCRS and a component of the NSW Primary Industries Climate Change Vulnerability Assessment (VA). In 2019 an internal desktop review was undertaken (Clark et al., 2019), developing the broad objectives of this study:

- undertake an improved high-resolution projection analysis of drought risk under climate change at a regional to farm level across NSW, encompassing a number

of biophysical drought indicators spanning meteorological, hydrological and agronomic drought.
- undertake analysis of changes in risk (frequency, duration and intensity) from a characteristic drought sequence (for example, 2000-2020).

This technical report describes the research and development program that underpins these objectives.

Previous analysis of drought under climate change

The desktop review (Clark et al., 2019) provides an overview of previous global and Australian studies that have examined drought in a changing climate. The main insights from global-level studies are:

- in most areas around the world drought events are expected to increase in severity and frequency in the future, due to decreasing of regional precipitation and increasing evaporation (Sheffield et al., 2012; Dai, 2011; Sheffield and Wood, 2008; Seneviratne et al., 2012).
- Trenberth et al., (2014) identified that increased heating as a result of global warming may not cause droughts, but it is expected that when droughts occur they are likely to set in quickly, be longer and be more intense. This concurs with previous global level investigation such as Sheffield and Wood (2008).
- the global climate drivers of variability and drought (teleconnections like the El Niño Southern Oscillation, ENSO, for example) are difficult to project under climate change because of uncertainties about feedback between the oceans and atmosphere.

The outcomes of global level studies also apply to Australia, where it has been identified that drought is likely to change based on future climate projections (Hennessey et al., 2008 , CSIRO and BoM 2015). Based on analysis of available observations, Nicholls (2004) identified that each drought was warmer than the previous drought arguing that their nature is shifting toward a more arid climate. Similarly, Bradley and Timbal (2008) identified that the severity of drought in Australia has been increasing given more intense and frequent hot days, heatwaves, and greater evaporation derived from changing climate.

Projections for southeast Australia so far also suggest that:

- it is likely to be warmer and drier (CSIRO and BoM, 2015), with more extreme fire-weather days (Hennessy et al., 2005).
- temperature is projected to rise across the region, with more hot days and fewer cool days, and increase the severity and frequency of fire weather with a longer fire season (Lucas et al., 2007).
- annual-average rainfall is projected to decrease in southeast Australia, with a greater frequency of severe drought and an increase in drought proportion (with

high confidence) compared to the rest country of Australia (CSIRO and BoM, 2015).

Based on CMIP4 models, CSIRO and BoM carried out a comprehensive projection analysis of meteorological drought at a 50km ~ 200km resolution. In summary, the results demonstrated that drought proportion is projected to increase [high confidence] over southern Australia, while there is an increase at medium confidence for the rest of the country. The exception is northern Australia where the increase has a low confidence (Gallant et al., 2013; CSIRO and BoM, 2015). Kirono et al., (2020) repeated many features of this meteorological drought projection using CMIP5 projections and found that the majority of models project an increase in drought severity, although there is a wide range.

Methodology

Overview

This section outlines the methodology used to develop the scenarios of future regional drought for NSW. It is structured around the flow chart in Figure 2 where the main elements of the computational projection system that was developed to produce the future scenarios are identified. The core aspects of the methodology are the biophysical modelling and drought indicators developed for the Enhanced Drought Information System (EDIS), with additional features like climate projections, downscaling as well as extended drought characterisation and analysis.

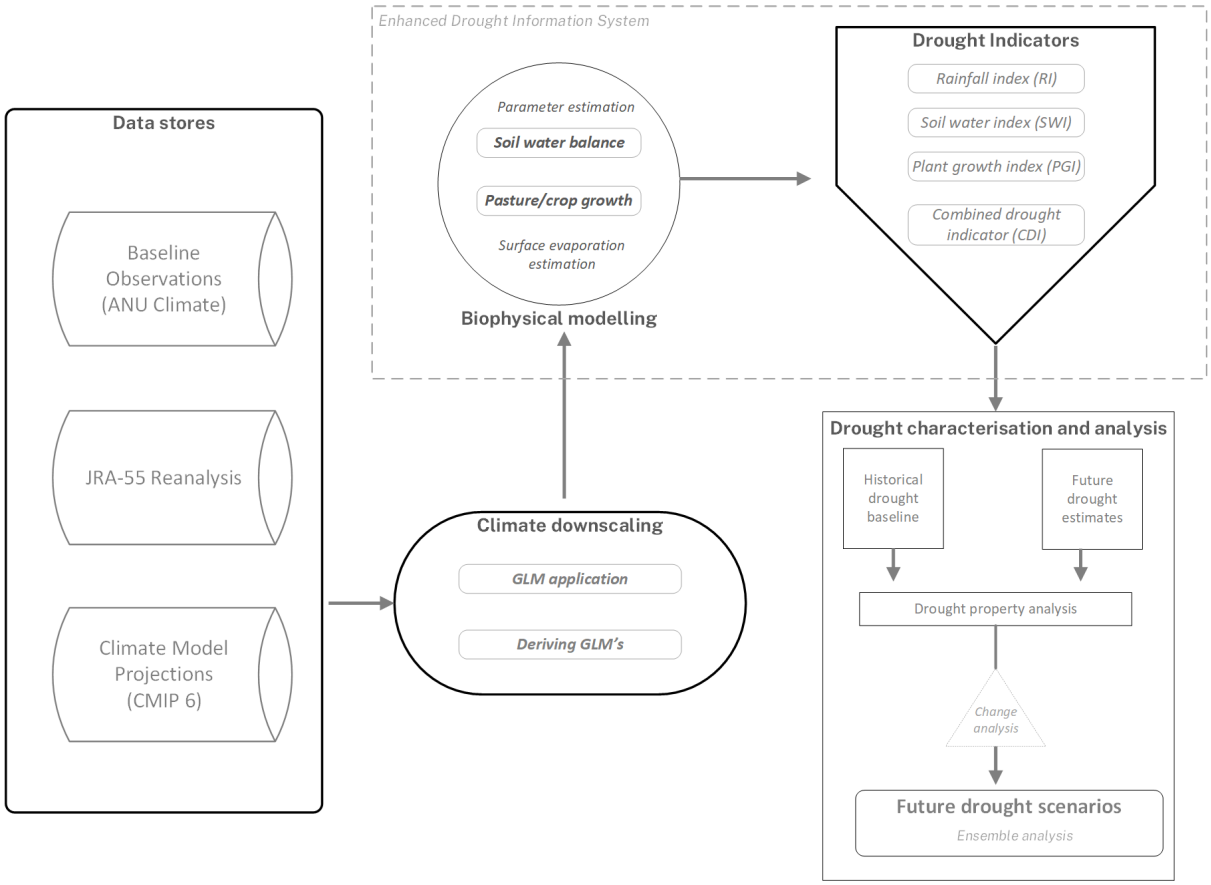

Figure 2. Main elements of the computational projection system used to generate future drought scenarios for NSW regions.

The projection system is an example of a top-down loosely coupled modelling framework. Different data sets, climate, biophysical and empirical models are integrated, but there is no feedback between the main elements. This is particularly important when considering the interactions between the landscape and climate system through the process of evapotranspiration, which can modify properties of drought events at micro and meso-scales. The use of empirical methods to downscale climate variables also brings the prospect that non-stationarity may influence the results, where models built on past relationships have limited ability to project dynamics as systems

change in the future. The modelling system used here contrasts with tightly coupled modelling frameworks, like full land-surface schemes or mechanistic agricultural models. The approach taken here needs to be considered as one that is practical but has limitations revolving around stationarity and system dynamics. There is value in the approach, but there is equal merit in pursuing analysis of a complex phenomenon like drought using alternative methodologies.

General design of the regional drought scenarios

The methodology is outlined in detail in the sections below, providing additional information about each of the main elements in the framework. In summary the general design features of the future scenarios include:

- the modelling and analysis were performed on a 1km^2 regularised grid across NSW.
- drought characterisation involved the calculation of four statistical properties of drought risk and exposure ('drought climatologies'). This includes the frequency, average and maximum duration and time spent in drought.
- changes in these metrics are determined from a 20-year base period (1995-2014) for near future (2041-2060) and far future (2081-2100) time slices.
- the changes in the future time slices are analysed for low (SSP245) and high (SSP545) global emissions scenarios.
- drought metrics and changes are calculated for a 26-member Global Circulation Model (GCM) ensemble sourced from the CMIP6 inter model comparison experiment.
- changes in drought metrics are reported for the ensemble mean using two approaches to summarise the 26-member model ensemble,
    - the first is a weighted approach which accounts for GCM quality (skill and independence),
    - the second is an unweighted method where all GCMs have an equal bearing on the reported mean.
- two methods for calculating potential evaporative demand (PET) at the crop/pasture-atmosphere boundary layer are used. This includes the Hargreaves-Samani and Penman-Monteith methods.

Computation

The computation projection system was implemented on a Linux cluster with the main processing modules developed in MATLAB™. The system runs in parallel, given the computational demand associated with high spatial resolution modelling and drought analysis across a 26-member model ensemble. Key tasks to enable parallel processing

included the development of custom data storage objects, developing an optimal chunking strategy suitable for the available computing resource, as well as re-engineering some model source code for processor threading. Generally, out of storage (in-memory) calculation strategies were implemented to maximise computational efficiency. Although only briefly summarised in this report, the computational engineering aspects of the project were critical to its successful completion, drawing on the time and specialist expertise of the project team.

Data stores

Baseline observations

The gridded climate data used in this study is produced for Australia by Hutchinson et al., (2021) and known as ANUClimate[2]. Station observations of daily climate variables are quality controlled and interpolated to a regularised 1km^2 grid utilising improved Laplacian thin plate smoothing splines (known as ANUSPLIN). Variables include daily rainfall, temperature (maximum and minimum), radiation, vapour pressure and potential evaporation from the Class A pan evaporation network. This produces a quality-assured observational data model at moderate-to-high resolution (1km^2). It is utilised in this work to construct the downscaling scheme, evaluate the robustness of projections and provide a baseline for comparison.

Climate model projections

Climate projection data was sourced from the sixth Coupled Model Intercomparison Project (CMIP6), basing this study on the most up-to-date ensemble of available future climate projections produced by the international community. This consists of quality-assured output files from the 26 selected GCMs from the endorsed Scenario Model Intercomparison Project experiment (ScenarioMIP, Tebaldi et al., 2021). This study accessed historical climate as well as future projection climate data generated by the models. The future climate data used in the study are from the Tier 1 (high quality controlled) model runs, focused on the SSP245 and SSP585 greenhouse gas scenarios designed by O'Neill et al., (2016).

Originally the model output files used in this study were sourced from the Australian node of the Earth System Grid Federation (ESGF) CMIP6 data archive, which is held on the National Computing Infrastructure (NCI). During the development of the downscaling methodology, further climate model output variables were needed. Additional data were obtained to support this study from the centralised European node of CMIP6. These additional variables are now available for Australian researchers on the NCI. Details of the final set of climate variables sourced and used in the study are provided in Appendix 1.

[2] https://openresearch-repository.anu.edu.au/handle/1885/147476

A custom data store was created locally where the GCM output files were further processed. The primary GCM data were:

- analysed and quality assured for completeness in time and space.
- clipped to the bounding box of the downscaling scheme.
- converted to the standard meteorological physical units.
- converted to the Gregorian (standard) time model.
- re-gridded from their native model geospatial scheme to a scale termed the 'common GCM spatial scale' used in this study.
- converted to the formats and data objects used in this study.

This created a consistent and complete GCM ensemble of daily predictor variables from 1970-2100 for utilisation in the downscaling scheme. Further technical detail is provided in the appendix on Empirical Statistical Downscaling.

JRA-55 Reanalysis

To develop the downscaling scheme, extensive three-dimensional climate observations at the common GCM spatial scale were sourced from the JRA-55 reanalysis[3] repository produced by the Japanese Meteorological agency. The JRA-55 reanalysis is the latest data assimilation scheme where observations and a highly constrained GCM are used to reproduce recent historical climate in time and three-dimensional space, including vertical atmospheric layers. Similar to the CMIP6 repository, this data was audited and reprocessed into the necessary formats and data objects so it could be effectively utilised to develop downscaling equations.

Climate downscaling

An Empirical Statistical Downscaling (ESD) methodology was developed to translate the projections at the GCM scale to the variables that are used for biophysical modelling and drought characterisation at the 1km^2 grid scale. A full description of the downscaling methodology development and evaluation is in Appendix 1. The decision to develop a custom ESD scheme was based on a number of considerations:

- at the time of development outputs were available from a regional climate modelling framework (NARCliM version1) based on CMIP 3 models, with updates scenarios for south-eastern Australia based on CMIP6 models in production but unavailable for this study.
- other readily available climate projections known as the NRM projection set are based on CMIP 5 and available for seasonal or monthly change fields, and were not fully suitable for drought risk assessments.
- the biophysical modelling framework in EDIS uses moderate to high accuracy daily climate fields that need variability at this temporal scale to be captured as well as cross variable correlation to be preserved,

[3] https://jra.kishou.go.jp/JRA-55/index_en.html

- this places distinct quality requirements on climate forcing data where, for example, the application of the available NARCliM RCM fields would have required development of a sophisticated bias correction scheme.
- the rainfall field is of particular importance in a drought study, and an assumption was made that basing the work on a large ensemble of new CMIP6 climate model runs should provide an improved estimate of this field compared to the available CMIP3 and CMIP 5 ensembles in Australia.

Deriving Generalised Linear Models

The Generalised Linear Modelling (GLM) framework was adopted, one of the many approaches to ESD that can be used (Benestad et al., 2008, Benestad 2001). As described and implemented in Timbal and Jones et al., (2008), GLMs have been used for this purpose in both Australia and internationally by a number of authors since the late 1990s.

In most previous applications, GLMs have typically been used to downscale GCMs to a limited set of individual climate stations (see, for example, Timbal and Jones et al., 2008). Appendix 1 outlines work carried out that extends GLM approach to downscale GCM outputs to the continuous 1km^2 grid across NSW. This involved computational development to partially automate the selection of candidate predictors for the GLMs and step-wise fit over a million GLMs, one for each 1km^2 grid cell of NSW. It also included developing an approach that addressed potential spatial discontinuity in the parameter estimation.

Application of Generalised Linear Models

Once derived, the parameters of the GLM models are stored in a specialised data object so they are available for production of scenarios. They are applied, given the data from each GCM or the JRA reanalysis, to produce climate change scenarios for rainfall, minimum and maximum temperature, radiation and vapour pressure at a daily time step on the 1km^2 NSW grid. These historical and projection series span 1970-2100 for the 26 models under the two future climate forcing scenarios. This data is used in the next steps where to drive EDIS and produce change analysis of future drought as well as for evaluation of the overall performance of the approach.

Biophysical modelling

DPI AgriMod is the biophysical model used for operational drought monitoring in the EDIS framework. It is a state-wide water balance, pasture and crop modelling framework that can be run in near real-time with daily, weekly or monthly gridded climate data. The model is a simple force-restore water balance which is structurally similar to WATBAL (Hutchinson pers com 2008) but uses layer calculations described by Rickert et al., (1998); a simplified biogeochemical growth model where the Gross Primary Productivity (GPP) equation of Kirschbuam (2015) has been modified for grasses, using the Growth Limiting Factor approach described by Nix (1981) for the

GROWEST model; and a temperature-radiation crop development function (based on Li et al., 2012 and Holzworth et al., 2015).

A sophisticated model optimisation procedure, using genetic algorithms and a finite difference approximation, calibrates the soil and pasture subroutines of the model across the NSW spatial domain. The optimisation fits the model to a high-quality but shorter-term estimates of plant GPP derived from the 250m^2 MODIS data (Donohue et al., 2014). Later versions also utilise satellite derived surface soil water products from NASA. Using the latest data allows key response systems to be parameterised based on the latest biophysical constraints and land use.

This provides an objective approach to estimating critical thresholds that underpin some of the main farming system responses to climate variations: the temperature-dependent photosynthesis response of crops and pastures, for example, or the tension at which water is held at on the soil matrix for root-phloem-leaf transpiration. This is a different methodology than employed in the main CCRS vulnerability assessment which used a-priori strategies for estimating these critical thresholds.

Calculation of evaporation

This study evaluated a number of methods for calculating the maximum potential exchange of water from pasture-crop canopy and surface soil to the atmosphere, or Potential Evaporation. This evaluation was undertaken because of the potential for PET methodologies to introduce bias in a projection study of drought under climate change. This issue, and methodological work undertaken for this study, is fully described in Appendix 2. To produce the future projections two methods have been used, the Hargreaves-Samani and the Penman-Monteith equations.

Drought indicators

Daily rainfall, plant available soil water and crop/pasture growth rates are retained from the biophysical model and used to calculate drought indicators. Each day is percentile ranked relative to the historical baseline to determine the Rainfall Index (RI), Soil Water Index (SWI) and Plant Growth Index (PGI). These are then integrated into a single metric of drought, the Combined Drought Indicator (CDI).

Percentile based indices have been chosen from a wide range of available drought indicators used by the global drought monitoring community (for overviews, see Clark and Mullan 2011; White and Walcott 2009; Wilhite and Sivakumar et al., 2014). Percentile-based indices involve ranking a period of interest relative to those experienced in the past (Gibbs and Maher 1967; White and Bordas 1998; Mpelasoka et al., 2008). The approach has been well tested in Australian conditions (Gibbs and Maher 1967; White and Bordas 1998) and is used in EDIS because they are widely understood by stakeholders in Australia. The individual indicators include:

- Rainfall Index (RI) - Meteorological Indicator: the RI is the percentile rank of daily rainfall data summed over a 12 month aggregation window and then ranked within the baseline of 1981 - 2020. The practical calculation across millions of grid cells is achieved by a computationally efficient method, where data are ranked in cumulative distribution functions rather than tied ranks of actual historical data. The RI is an index between 0 and 100, where, for any given climatic environment, values approaching 0 are close to the driest on the historical record, and those approaching 100 are close to the wettest.
- Soil Water Index (SWI) - Hydrological Indicator: the SWI is calculated using the same procedure as the RI but uses a soil moisture field derived from the DPI AgriMod soil water balance. Here, the plant available soil water from layer one (0-10 cm) and layer two (11-45 cm) are aggregated and used. This has advantages as it includes the processes of evaporative demand and rainfall-runoff, thereby accounting for rainfall effectiveness for production.
- Plant Growth Index (PGI) - Agronomic Indicator: the PGI is also calculated using the same procedure as the RI but uses the relative crop/pasture growth output from DPI AgriMod. If the predominant land use is cropping, according to the National Dynamic Land Cover Dataset[4], the PGI uses the crop model output. Otherwise, it is calculated using the pasture model output. The PGI is an agronomic drought indicator which is not only sensitive to soil moisture but also seasonal temperature variation, events like frosts, as well as the radiation budget.
- Combined Drought Indicator: The individual drought indices are integrated into a single index of drought status (CDI). The CDI was developed to integrate the 'multiple definitions' of drought that underpin the individual indicators. The use of a standard scale in the individual drought indicators (percentiles from 0-100) supports a straightforward approach to integration, with no need for re-scaling or a-priori weighting schemes. The CDI adopts the approach described by Svoboda et al. (2002) and Sepulcre-Canto et al. (2012) and applies decision rules and thresholds to group conditions into different phases. The phase terminology and choices around thresholds were developed and refined iteratively through stakeholder engagement.

When all indices are below the 5th percentile level, conditions are classed as 'Intense Drought'. If any of the indices are below the 5th percentile level, conditions are defined as 'Drought'. Conditions are 'Drought Affected' if one of the indices is below the 30th percentile. 'Recovery' occurs when all indices are above the 30th percentile and below the 50th percentile. The time series (Figure 3a) for South Casino in NSW provides an example of the CDI and individual indices since 2016. A map of drought intensity on the 30th of November 2019 is in Figure 3b. These are examples of the routine near real-time

[4] https://www.agriculture.gov.au/abares/aclump/land-cover/dynamic-land-cover

analysis delivered to the public as web services that also inform the monthly State Seasonal Update[5].

The key outputs from EDIS used in this study are the Rainfall (RI), Soil Moisture (SWI) and Plant Growth (PGI) drought indicators. Here the minimum of the indices is taken, and the 10th percentile used to indicate a drought event. This is equivalent to calculating the Drought or Intense Drought categories of the Combined Drought Indicator in the operational framework. This study relaxed the threshold from the 5th percentile used operationally to the 10th percentile. This was done as a way to account for noise in the meteorological indicator to improve the stability of the additional drought metric calculations.

[5] https://www.dpi.nsw.gov.au/dpi/climate/seasonal-conditions-and-drought/nsw-state-seasonal-update

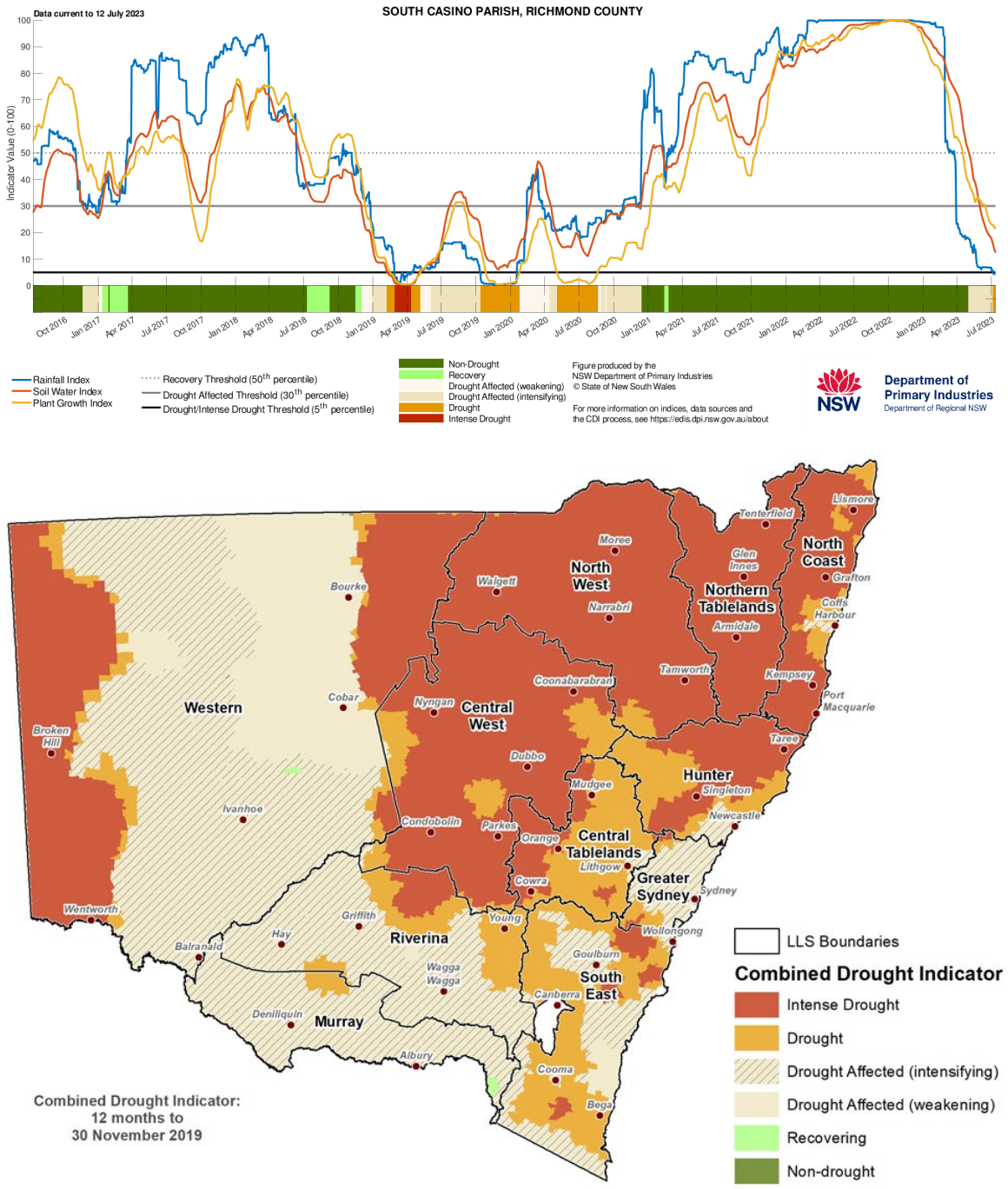

Figure 3. Examples of (a) the individual drought indicators and CDI time series at a specific location and a map of the CDI for 30 November 2019.

Drought characterisation and analysis

Drought property analysis

Droughts are multi-dimensions events, with key partially correlated properties like ‘frequency’, ‘duration’ and ‘intensity’ that need to characterised to provide a full assessment of risk. A formal statistical analysis of drought climatology for a given site or region accounts for the multidimensionality through the use of bi-variate and, in some cases, tri-variate probability density functions. The shape and correlation structure of the function provides a ‘characteristic drought’ profile. Drought risk is depicted by the shape and properties of the function and will, for example, differ across regions within NSW and for climatic zones around the world. The aggregate risk of drought is determined by integrating the area under the probability density function.

To illustrate this concept the characteristic drought for NSW is provided in Figure 4. This example was constructed by aggregating the CDI across the state by calculating the extent (land area) and duration (days) of drought events from 1980-2020. The probability density function fitted to these calculations (Figure 4) indicates that the most common drought events last between 0.5 and 1 year (200-400 days) and affect between 20-40 percent of the state. There also are many other types of droughts that are less frequent: long duration (two years or more) events, for example, that have a wide extent, affecting 70 percent or more of NSW.

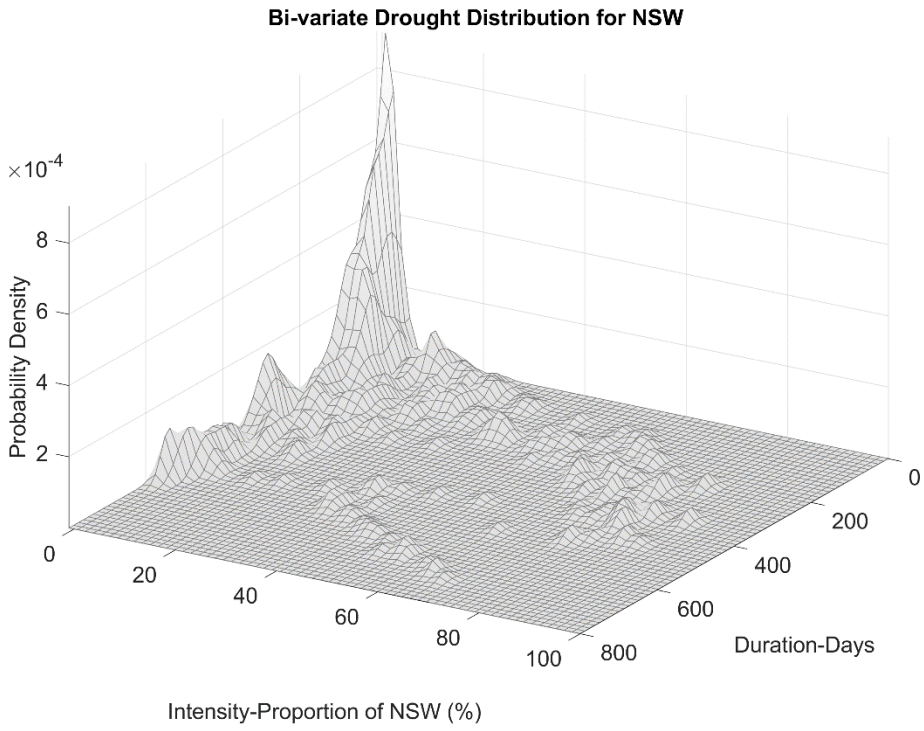

Figure 4. Probability density function or ‘characteristic drought’ for NSW. Determined by calculating aggregate duration and extent (proportion of NSW) of droughts using the NSW-CDI for 1980-2020.

While the bi-variate distribution in Figure 4 is an example of a full quantification of drought risk, it is often reported as separate constituent features for ease of communication with stakeholders. The regional drought scenarios produced for this study report on the following drought properties:

- average duration of droughts in days.
- maximum duration of droughts in days.
- number of drought events in a 20-year period.
- time spent in droughts as a percentage of a 20-year period.

Ensemble weighting

The four metrics that capture some of the main features of drought were derived for 26 GCMs for two evapotranspiration methods over a near and far future time slice. They are expressed as unit changes from a baseline threshold, the drought sequence from 1995-2014. A weighting scheme was developed so that the reported mean of the 26-member ensemble does not overtly reflect models that are performing relatively poorly in representing the variable of interest (drought metric), as well as not overtly weighting GCMs from a similar model family represented by an independence score. This approach was devised by Sanderson (2017) and its technical implementation is provided in Appendix 1.

Future Drought Scenarios

Baseline drought climatology

The baseline drought climatology statistics for the Hargreaves-Samani (HS) and Penman-Monteith constant wind (PM) PET methods are in Figure 5. The statistics are calculated for a 20-year base period from January 1995 – December 2014. These highlight that the characteristic drought profile changes markedly at a regional level across the state. The western precinct of NSW spends between 10-15 percent of time in drought. This is a relatively shorter period than some sub-regions of the eastern coastal fringe, particularly the south-east of the state, which spends over 20 percent of its time in drought. Close inspection of these areas highlights that this is likely due to topographic or rain shadow effects.

In the west and some regions along the coast the number of droughts is higher at almost 8 across the evaluation window compared to as few as 2-4 in central west of the state. The average duration is shorter in the west at 100-200 days, whereas some parts of the coastal fringe have and average duration of up to 500 days.

The maximum drought statistic has a degree of randomness and discontinuity in terms of its spatial distribution across NSW, particularly to the west of the state. This is because it is an extreme value calculation and subject to both the innate natural uncertainty in the climate system as well as error on the underlying data. The baseline case established by this data highlights long duration droughts between 500-1000 days are experienced across most of the state. There are geographically distinct sub regions where the maximum duration recorded is over 1000 days.

In terms of a reference baseline case, generalising across the state, NSW droughts typically have the following characteristics:

- an average duration of between 200-500 days, with events occasionally extending to up to 1000 days.
- The frequency of drought is moderate-to-high in NSW, with regions experiencing 4-8 drought events across a 20-year timeframe.
- NSW regions spend between 10-20 percent of their time in drought.
- The characteristic drought profile varies across NSW where:
    - The western region of NSW, characterised by high seasonal variability, experiences more-frequent shorter-duration droughts.
    - areas such as the central west and tablelands experience fewer droughts but they are typically longer in duration when they occur.
    - there are sub-regions where drought exposure increases markedly compared to the state and the surrounding climatic zone. In these areas, time spent is drought over a 20-year window may be 20 percent or more, they occur with moderate-to-high frequency with up to 8 events in this

management window and some of these events have long durations of 1000 days.

Interpreting the geographic distribution of these metrics, in particular those for the west of NSW, needs to consider the way the drought indicators are constructed and the natural climatic environment. The indicators account for periods of deviation (dryness, low soil moisture and poor growing conditions) relative to historical conditions in that region. They are not indicators of overall aridity. Western NSW is a low rainfall rangelands environment where long dry spells are a persistent feature. The distribution of daily rainfall is highly skewed, where falls over 20mm are infrequent within a season, usually a product of a storm or drift of a frontal system outside of its traditional path. Droughts in this part of NSW are events where a land area may miss these intermittent events. Typically a fall of this nature appears to be received every 300-400 days, leading to the lower average drought duration found in this part of NSW.

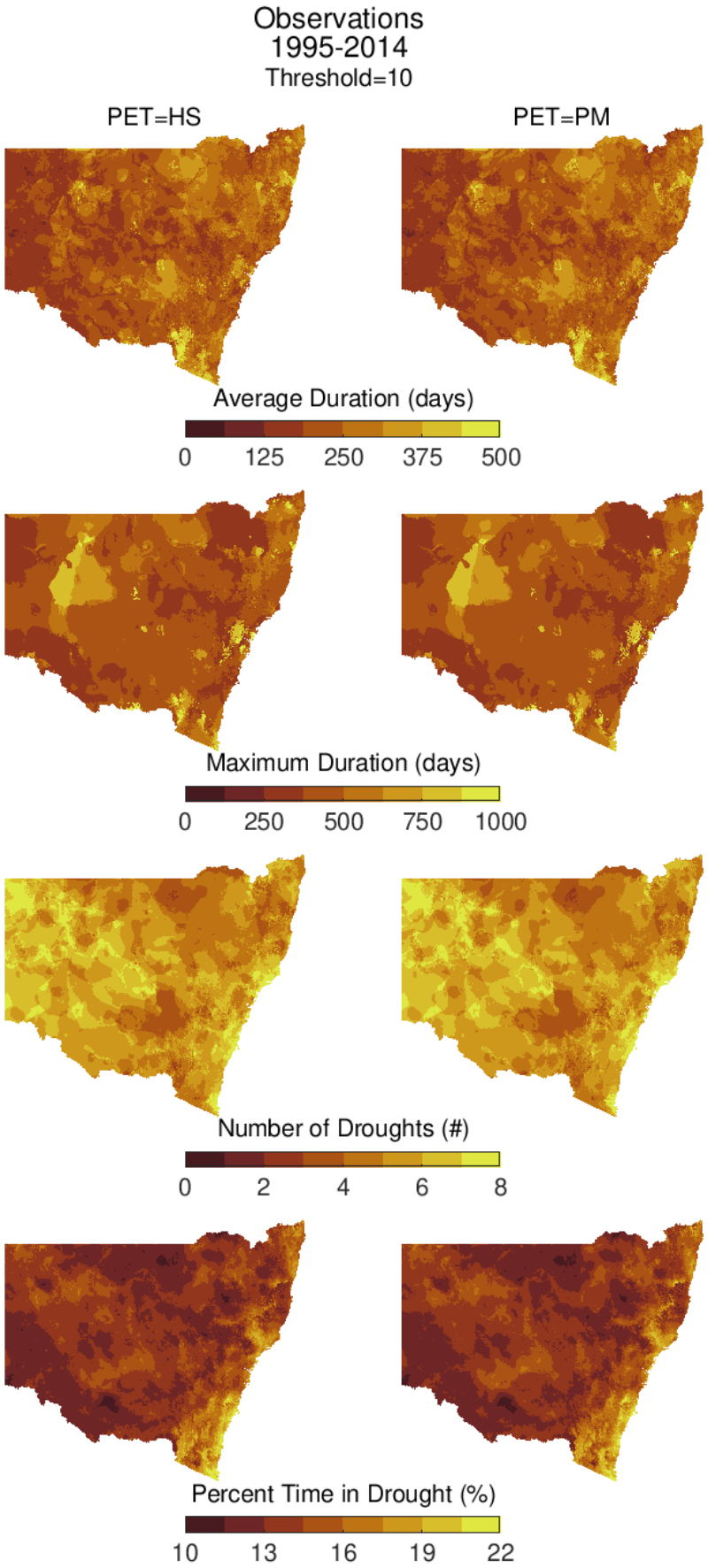

Figure 5. Baseline drought climatology for NSW showing different drought characteristics.

State-wide drought scenarios

High-level scenarios for future NSW drought are summarised in Figure 6-Figure 9. These maps present the weighted and unweighted multimodel mean (26 GCMs) for two emissions scenarios in the near future (2041-2060) and the far future (2081-2100). The mapped values are changes in key drought metrics from the 1995-2014 baseline.

The initial obvious interpretation, based on a state-wide examination of the maps, is that droughts appear to be getting worse across NSW in the future in all the key drought metrics. This holds for both the weighted and unweighted ensemble and the two PET methods. The interpretation below provides a more detailed assessment of the patterns over time for different emissions scenarios and focus points (drought metrics) of the characteristic drought profile. The interpretations focus on describing the weighted case for the HS PET method (Figure 6) as being representative of the wider results. Some important differences found between the GCM weighting schemes are discussed in more detail below.

Average drought duration

Average drought duration extends under the more conservative SSP245 emissions scenario as early 2041-2060, where in some areas, events last on average up to 100-200 days longer than experienced in the contemporary baseline. The most extreme regions of change appear to be concentrated in the central north west of the state and coastal fringe.

Within this overall trend, there are also regions where little change occurs, particularly the upper reaches of the Central, Northern and Southern tablelands. Here average drought duration stabilises and even reduces slightly under more extreme emissions scenarios in the far future.

The main effects on average drought duration appear to be proportional to both the emissions scenario and become more extreme over the course of the century. For example, average drought duration increases between 300-500 days in the far future (2081-2100) under the more extreme emissions scenario (SSP585).

Maximum drought duration

The effects on the maximum duration metric appear to follow a similar spatial and temporal pattern as described for average drought duration. Results for maximum drought duration indicate that an extra 100 -200 days could be added to the major 500-day drought events experienced in recent history. By 2100 the duration of these rare but extremely prolonged events would extend by multiple years – the extreme drought event of 2100 would be up to twice as long as a long drought in the baseline.

This metric is designed to provide insight into the changes the longest duration multi-year drought that could be expected in the 20-year window, compared to that of the contemporary baseline. As described for the baseline case, this metric has a degree of

randomness and instability. It should be considered the least reliable of the four metrics reported in this study.

Number of droughts

The number of drought events expected in a 20-year window appears to increase in some parts of NSW in the future. There are some zones where decreases occur, such as in the far west and north east of the state in the far future. This may be an artifact of the correlation of this duration and frequency of drought. As the forward climate scenarios become more extreme, droughts become prolonged multi-year events and they begin to merge and are counted as one event when accumulating the frequency statistic.

Despite this, the predominant trend is toward slightly more drought events over a 20-year window, up to three additional droughts, or for simplicity, approximately one more drought to manage per decade. It is important to recognise that this may be a short-duration, high-intensity event, like a flash drought event in coastal NSW.

Time in drought

This metric provides an approximate time spent in drought into the future, inclusive of all-drought types, be they long-duration low-intensity or short-duration high-intensity events. It is a metric that provides a holistic estimate of drought change.

The data provide evidence of drought increasing proportionally in line with the emissions scenarios and over the course of the coming century. Relatively small increases are evident in 2041-2100, with most areas of NSW experiencing 10-20 percent more time in drought. The percentage increases are slightly higher for the more extreme emission scenario.

Time spent in drought increases dramatically by the end of the century, particularly under the high emissions scenario. Here a 40-50% increase in the time spent in drought is expected in the north, north east and much of the coastal fringe of NSW. Other areas experience a 20-40% increase.

Within these main effects, there are sub-regions where the time spent in drought does not change substantively, even in the far future under the more extreme emissions scenario. This area is concentrated on the upper reaches of the NSW tablelands, extending along the spine of the dividing range which transverses NSW. This zone is in the high rainfall zone of NSW, where current climate is extremely wet and cool. It is likely that its unique typographic setting and aspect negates changes to rainfall simulated in the downscaling, as well as the effects of more general warming. It may become slightly drier, but in this environment, it does not lead to soil water and pasture growth deficiencies. In some cases, the temperature and hydrological regime becomes more optimal for growth. This type of effect is not without precedent, where other high-resolution impact assessments point to the creation of ‘refuges’ in some parts of the landscapes given aspect, topography and or soil types.

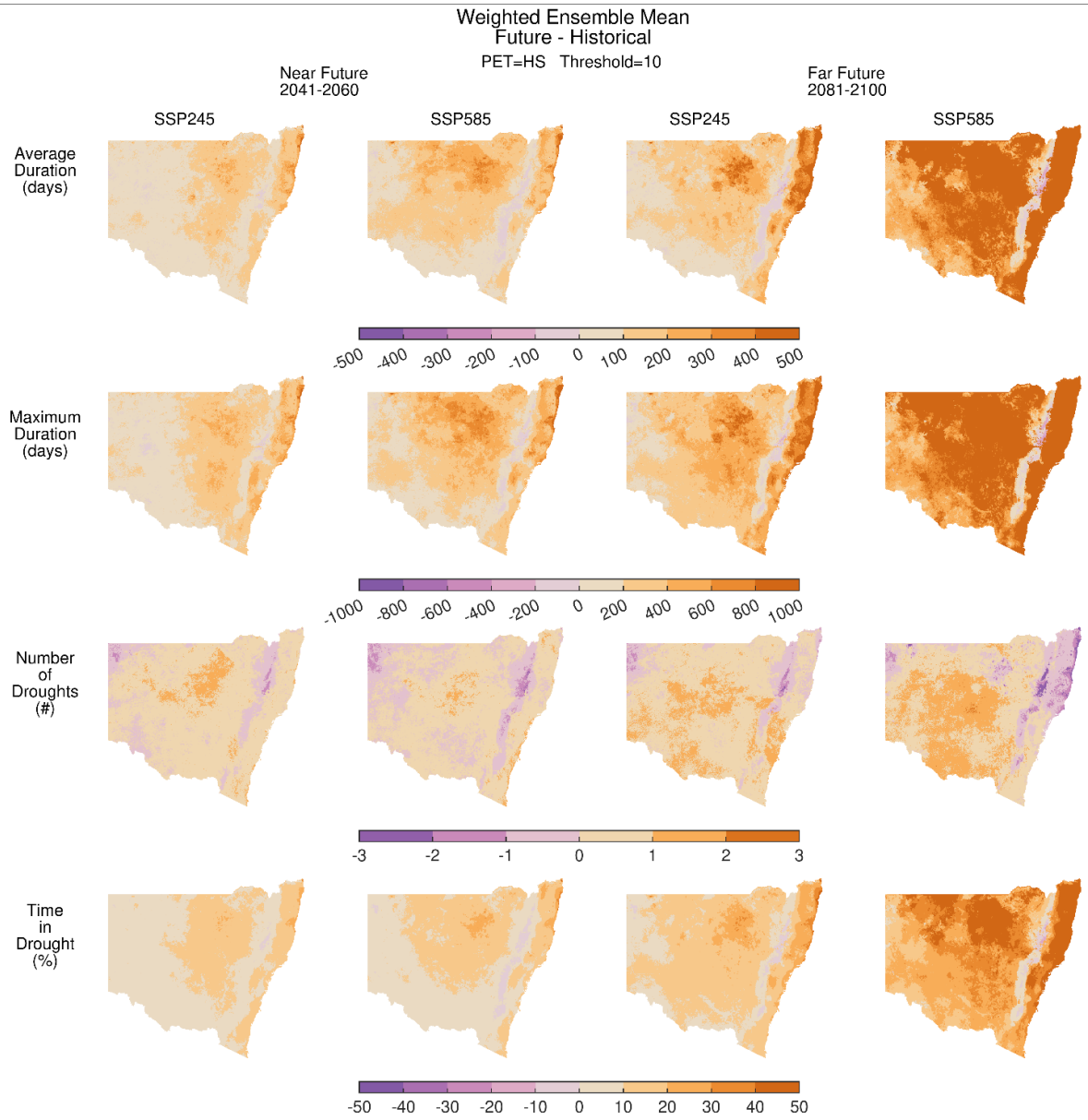

Figure 6. Regional to state-wide scenarios of drought for NSW showing the weighted ensemble mean for the Hargreaves-Samani (HS) PET method. Data in these maps are changes from the 1995-2014 baseline for key drought metrics: the time spent on drought (percentage of a 20-year period), number of droughts across the 20-year period, maximum duration of droughts (days) and the average duration of droughts (days).

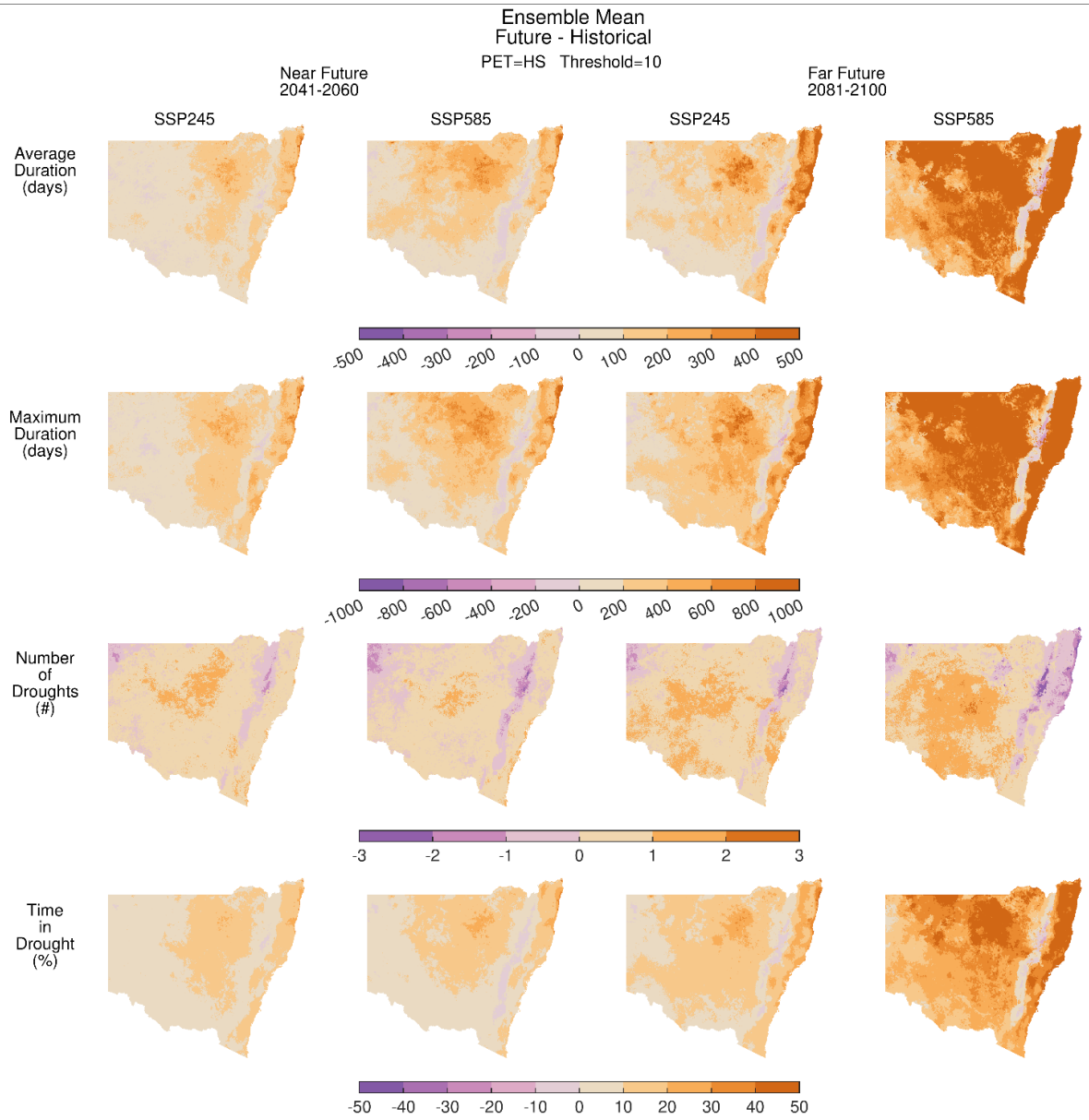

Figure 7. Regional to state-wide scenarios of drought for NSW showing the ensemble mean (i.e. equal GCM weighting) for the Hargreaves-Samani (HS) PET method. Data in the maps as per Figure 6.

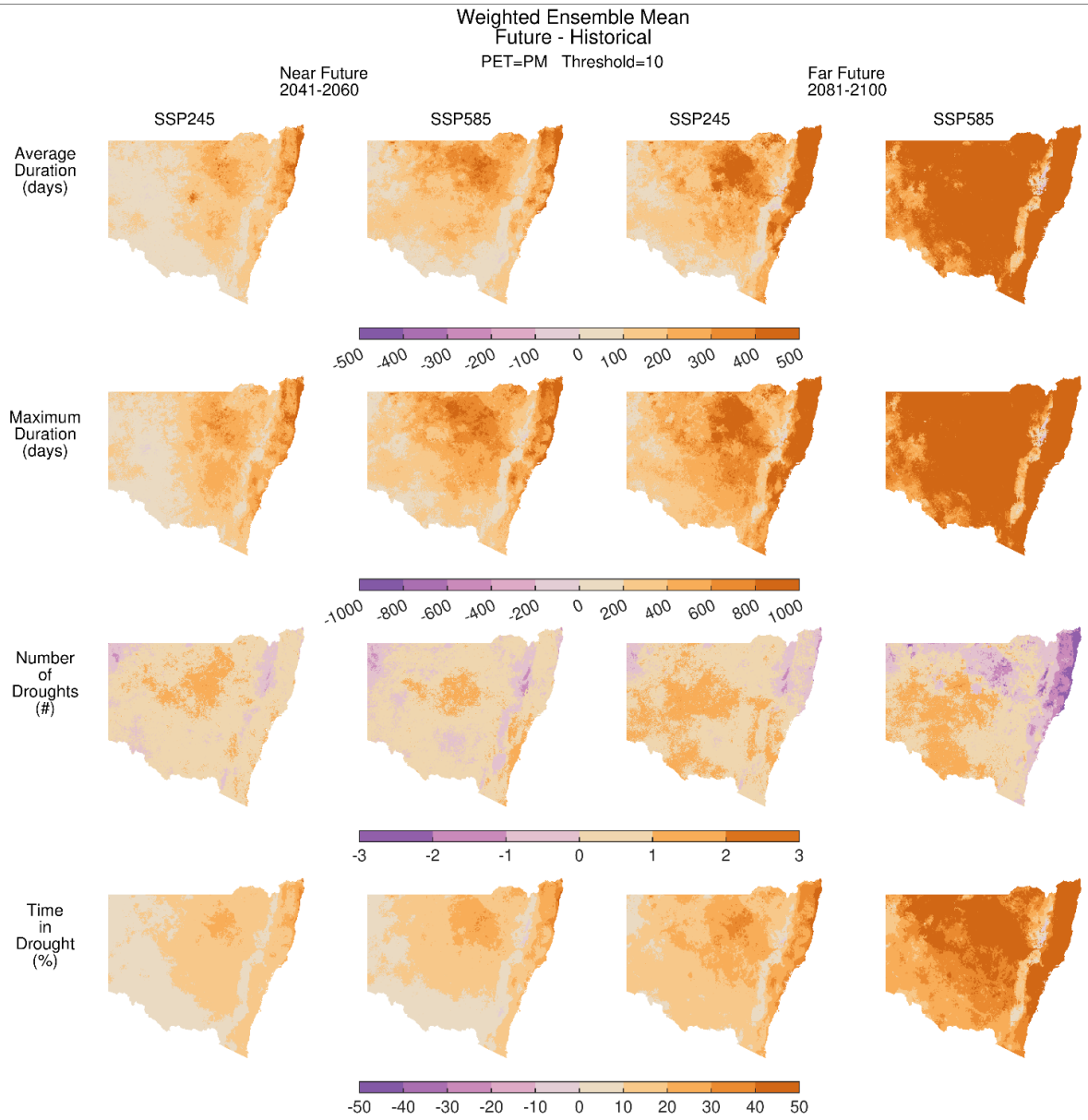

Figure 8. Regional-to-state-wide scenarios of drought for NSW showing the weighted ensemble mean for the Penman-Monteith constant wind (PM) PET method. Data in the maps as per Figure 6.

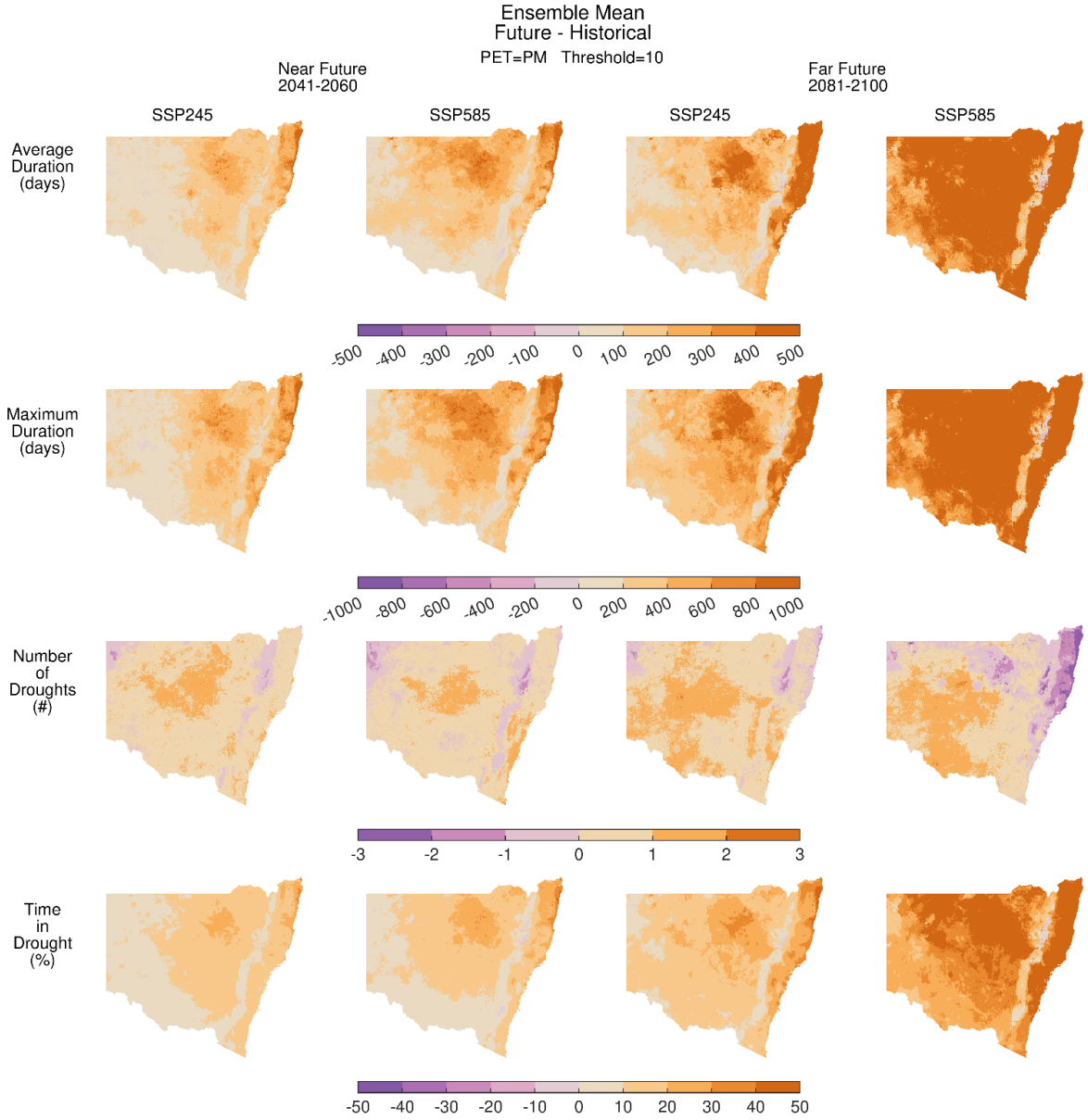

Figure 9. Regional-to-state-wide scenarios of drought for NSW showing the ensemble mean (i.e. equal GCM weighting) for the Penman-Monteith constant wind (PM) PET method. Data in the maps as per Figure 6.

The influence of GCM quality

A comparison of the weighted and unweighted GCM ensemble methods are presented for the HS PET method in Figure 10 and the PM method in Figure 11. The bottom panel in each figure is a simple change analysis where the unweighted method is subtracted from the weighted mean method (labelled 'Difference Weighted-Mean').

For much of NSW, particularly for the near future and under the low emissions scenario, there are negligible differences between these two approaches to analysis of GCM ensembles. The calculated difference is of the order of ±40 days, against a change signal of +100-200 days. For these cases, factoring in GCM quality appears to result in negligible differences and it is appropriate to construct general scenarios of drought utilising either method.

In contrast, for analysing GCM ensembles under a higher emissions scenario, particularly in the far future, weighting does appear to be important. Large differences between the weighted and unweighted methodology are evident particularly to the north and northern coastal fringe of NSW. Using the unweighted methodology would result in an underestimate of change to drought duration, in the order of 100-200 days, in these zones. This is against a projected change signal of 200-400 days, so an underestimation of 25-50 percent.

This result likely reflects the climatology of the region and the divergence in the ability of GCMs to capture the geographic patterns of sub-tropical processes at regional scales. Northern NSW is in the uniform to slightly summer dominant rainfall zone of the state where the latitudinal position of the South Pacific Intertropical Convergence Zone has an influence of the climatic regime. It is widely recognised that simulating the inter tropical convergence in GCMs is a key area of uncertainty, and as a result there is typically a wide inter model variance in ensembles in its summer latitudinal position. Projections of Australian rainfall built from the CMIP4, CMIP5 and now the CMIP6 model ensembles have considerable diversity in the north of NSW, with both positive and negative changes in averages for the summer season.

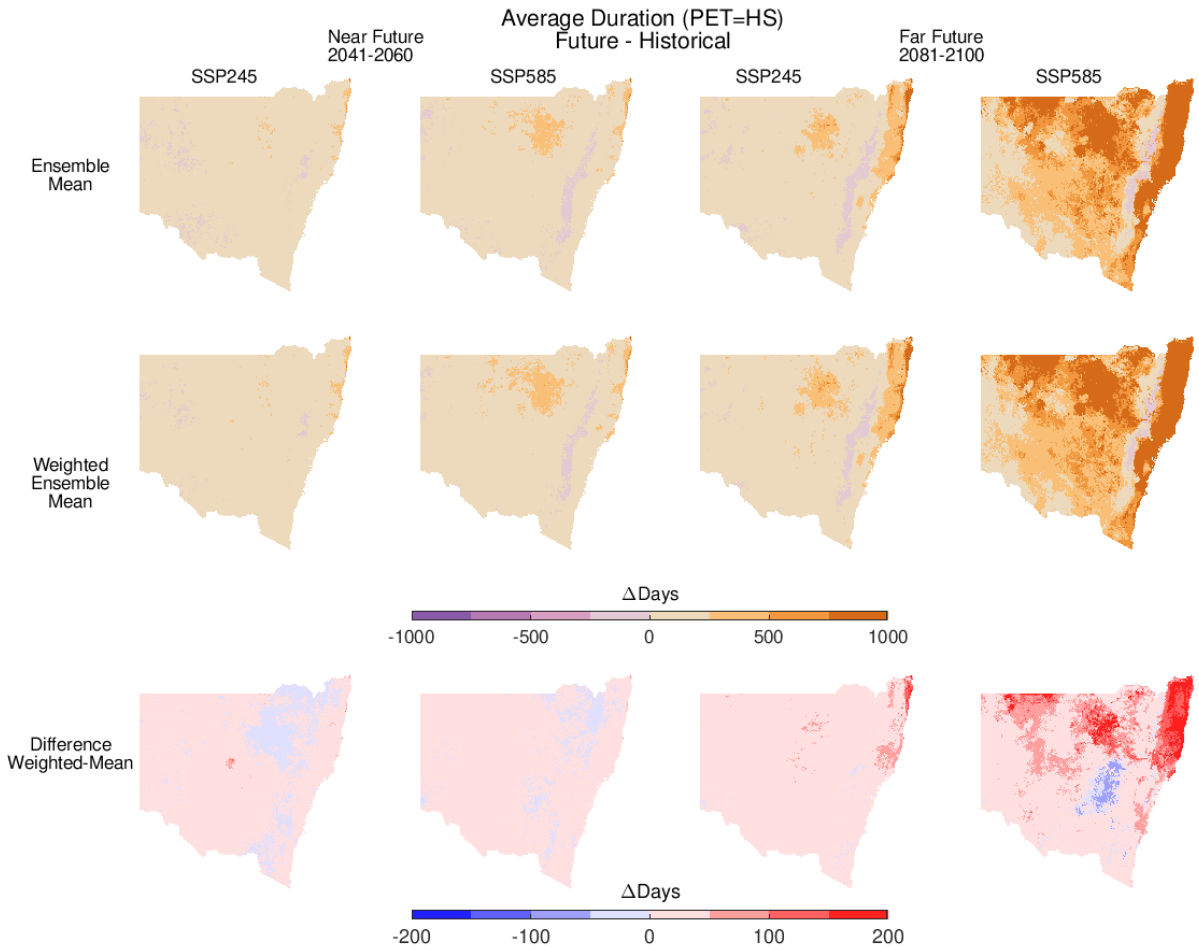

Figure 10. Comparison of the weighted ensemble and unweighted ('Ensemble mean') average drought duration change estimate for the Hargreaves-Samani (HS) PET method.

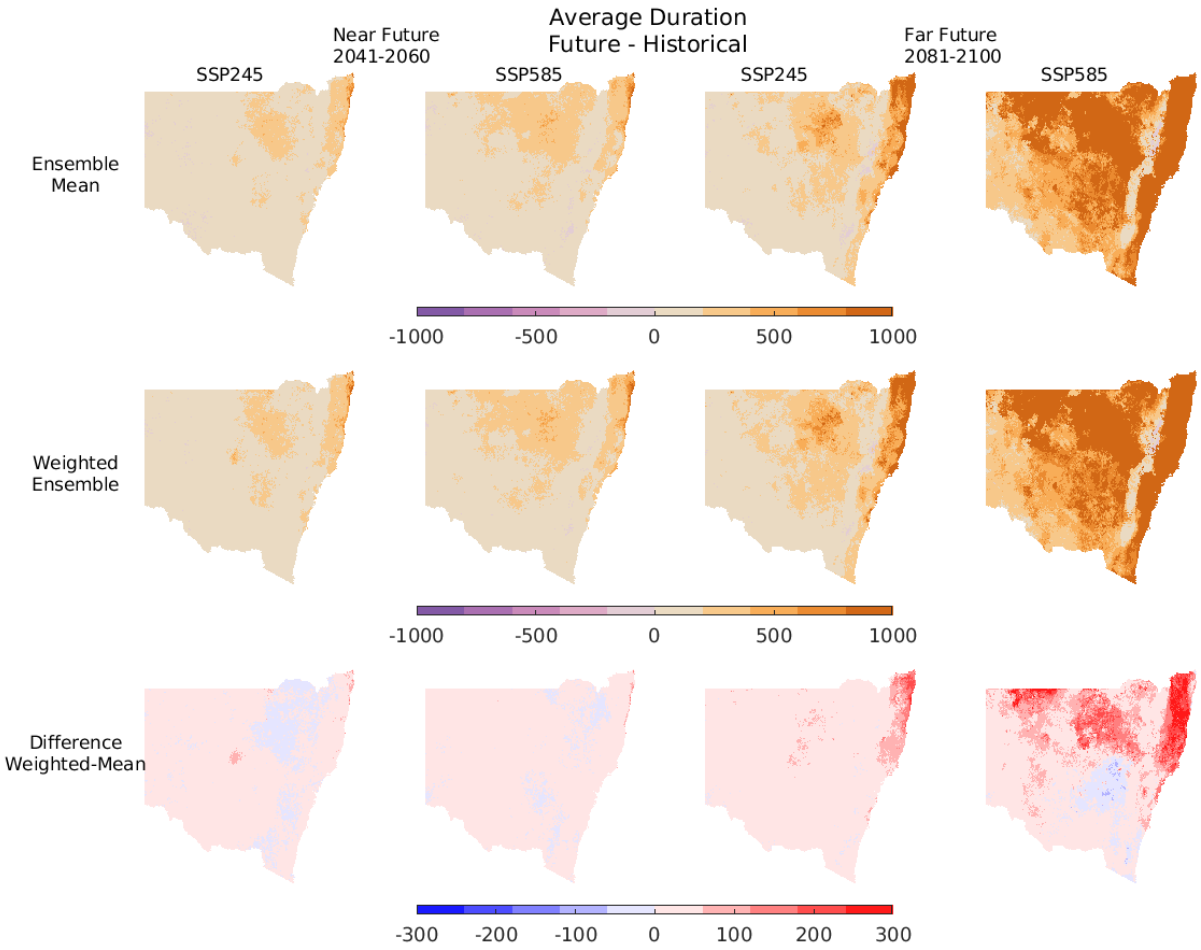

Figure 11. Comparison of the weighted ensemble and unweighted ('Ensemble mean') average drought duration change estimate for the Penman-Monteith constant wind (PM) PET method.

Appendix 1. Downscaled Regional Climate Scenarios

Summary

This appendix is for a more technical audience, describing the Empirical Statistical Downscaling (ESD) methodology used to develop the future climate projections, that in turn produce the NSW scenarios of drought.

The work described on ESD in this chapter is also a stand-alone study with the potential for applications beyond this particular drought analysis. The work contributes to the scientific field because it addresses a number of limitations that are evident in past applications of ESD in Australia:

It required the acquisition of additional fields from the CMIP6 model ensemble, with additional data now available to all interested researchers in Australia through the National Computation Infrastructure (NCI).

It included the development of a robust predictor selection methodology that minimises a-priori selection and spatial discontinuities in parameter estimation, thereby allowing the scaling of the scheme to produce continuous gridded projections across the state at 1km^2. This is equivalent to the production over a million individual climate station projection sets.

The ESD scheme was developed as a pragmatic customised approach for the purpose of projecting future drought. It was pursued in full knowledge of its potential limitations, in particular the potential for non-stationarity. The lack of feedback between the earth surface and climate system at regional scales, for example, could affect projected regional patterns of change. It is important to identify for the reader that the type of downscaled projections developed for the purpose of this study are unique, and as such other approaches have an equally valid contribution. Readers are strongly encouraged to examine work and projections that utilise alternative methods of dynamic downscaling of Regional Climate Modelling, in particular the NSW NARCliM program [6] (Evans et al., 2014).

Empirical-statistical downscaling (ESD)

Statistical downscaling took place in two multi-step parts. In the first part, predictors are selected from a gridded reanalysis data set (JRA), and the downscaling models are built using Generalised Linear Models (GLMs) to predict five climatic variables of interest (predictands) to drought modelling. The predictors were linked to historical

[6] https://www.climatechange.environment.nsw.gov.au/climate-projections-used-adaptnsw

observations of the predictands from the ANUClimate dataset to build the predictive models.

Table 1. Predictands in this study, the five daily climatic variables that are used in the Enhanced Drought Information System (EDIS) to model soil water and plant growth responses, and subsequently construct drought indices.

Abbreviation	Description
tmin	Daily minimum temperature recorded (°C), measured at 1.5m from the surface. From 12am-12pm.
tmax	Daily maximum temperature recorded (°C) measured at 1.5m from the surface. From 9am-9am.
vp	Vapour Pressure (hPa, hectopascals). Average 9am-3pm average derived from dew point temperature.
rad	Downwelling surface radiation (MJ/M2/day)
rain	Daily rainfall accumulation (mm) in a gauge at 1.5m from the surface.

In the second part of the methodology, future projection data from CMIP6 is run through the calibrated GLM downscaling models to generate projected downscaled climate variables. These downscaled variables are then run through the EDIS drought framework, starting with the soil water balance model, DPI AgriMod, followed by a percentile ranking step to produce drought indices. In this specialised run of DPI AgriMod, potential evaporation is estimated using both the Hargreaves-Samani and Penman-Monteith equations, the latter forced with a 2 m/s constant wind. For more information on the sensitivity of drought to different PET equations, see Appendix 2.

Processing of the GLMs for each variable was conducted on a virtual Linux operating system using MATLAB R2019a (The Mathworks Inc., 2019). Two machines with 48 CPUs and 360GB RAM each were used to process multiple variables and chunks at once. To facilitate efficient processing, the data was processed simultaneously in geographic chunks according to the size of the JRA grids. The ANUClimate data was saved as discrete chunks in native MATLAB format (i.e., matfiles) corresponding to the JRA grid in which the ANUClimate data was located. This enabled the chunks to be processed in parallel using MATLAB's Parallel Computing Toolbox.

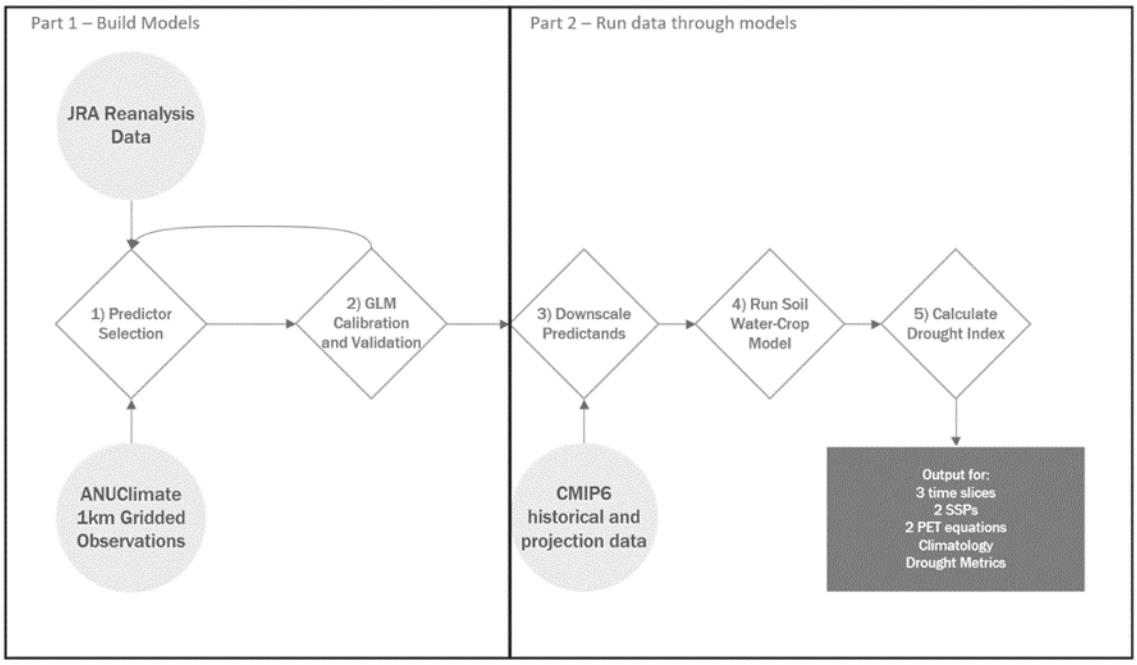

Figure 12. Overview of the Empirical Statistical Downscaling (ESD) and drought estimation scheme developed in this study.

Predictor selection

Predictors were selected in a two-stage process that included a pre-screening cross-correlation analysis with up to 2-day lags, followed by a manual backward elimination. Prior to this formal predictor selection step, the candidate predictors from the JRA reanalysis were audited to ensure that they were also available across the CMIP6 ensemble. For rainfall occurrence, the pre-screening process used distributions of the predictors categorised by occurrence or non-occurrence of rainfall. Predictors that showed distinct distributions between occurrence and non-occurrence were retained for the stepwise logistic regression.

Table 2 provides the full set of predictors that were subject to screening and selection process. The final set of predictors used in the next stage of model calibration are in Table 3.

In the first step of predictor pre-screening for all variables other than occurrence, the cross correlation between the observed variable and the predictors at the nearest JRA grid point was calculated for 3 lags (0, 1, and 2 days) for each of the 27 predictor variables and 939,526 observational grid points. Figure 13 is an example of the pre-screening process for daily maximum temperature. At each grid point, the maximally correlated lag from each predictor was noted. In order to have consistent predictors across the state, the predictor-lag combinations that occurred most commonly across grid points (>33%) were retained (Figure 13; left). In the next step, the mean spatial correlation of all the remaining predictor-lag combinations was calculated and predictors with correlations >0.4 at the 5% significance level were retained (Figure 13; right).

Table 2. The full set of predictors that were obtained for this study where there was availability across both the JRA reanalysis and the CMIP6 model ensemble. Naming conventions follows the metadata of the CMIP6 ensemble archive.

Abbreviation	Description
hurSfc	Near surface relative humidity
taSfc	Newar surface air temperature
psl	Sea level pressure
uaSfc	Eastward near surface wind
vaSfc	Northward near surface winds
zg850,500	Geopotential height at 500 and 850 hPa
hus850,500	Specific humidity at 500 and 850 hPa
hur850,500	Relative humidity at 500 and 850 hPa
ta850,500	Air temperature at 500 and 850 hPa
ua850,500	Eastward near surface wind at 500 and 850 hPa
va850,500	Northward near surface winds at 500 and 850 hPa
wap850,500	Vertical atmospheric flux (Omega) at 500 and 850 hPa
rlds	Surface downwelling long wave radiation
rsds	Surface downwelling short wave radiation
hfls	Surface upwelling latent heat flux
hfss	Surface upwelling sensible heat flux
clt	Total cloud cover percentage
rlus	Surface upwelling long wave radiation
rsus	Surface upwelling shortwave radiation

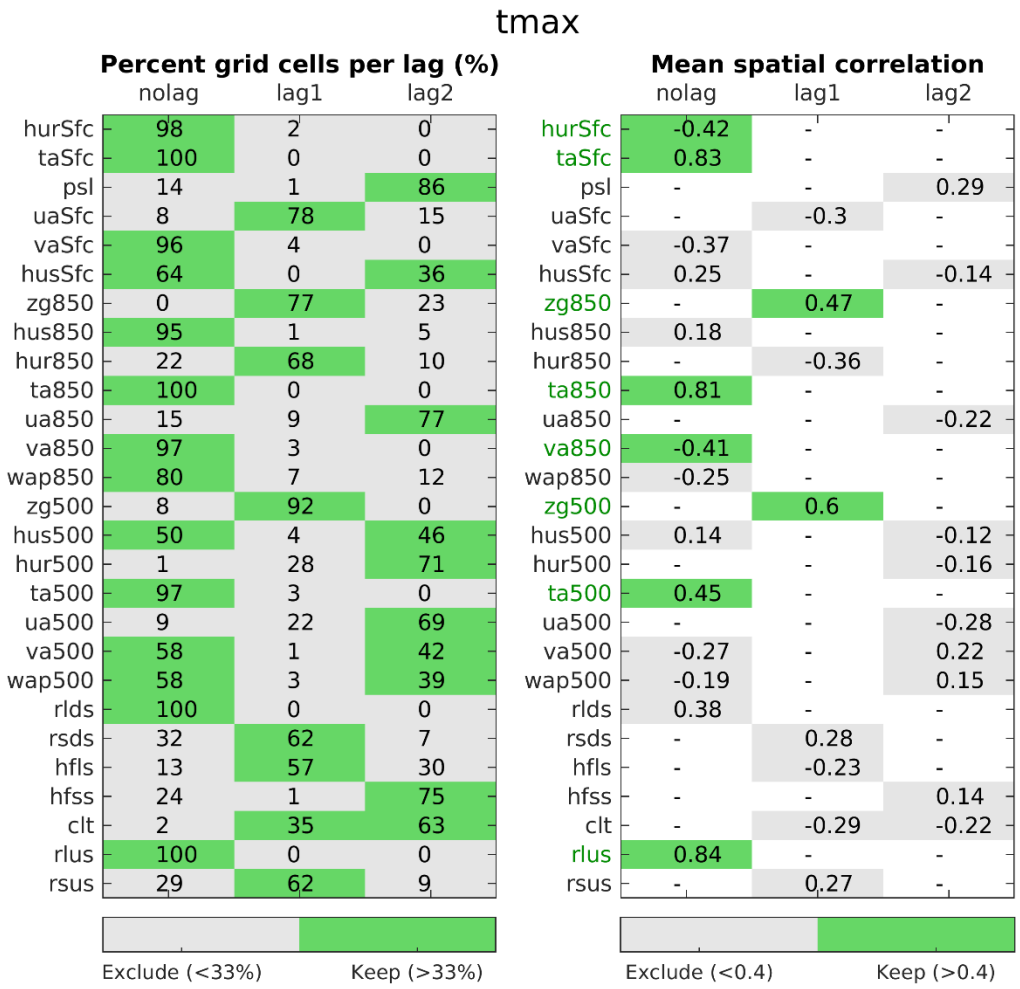

Figure 13. Example of pre-screening process as applied to maximum temperature (tmax). Each row is a predictor and each column represents the 3 lags of that predictor. (left) The numbers represent the percentage of grid cells (n=939,526) where a given lag held the maximum correlation. Lags represented in more than 1/3 of grid cells were retained (green) for the next process of screening. In some cases, two lags were retained for a given predictor. (right) For the retained predictors, the maximum correlation from the first step's cross-correlation was used to calculate the mean spatial correlation between the predictor and predictand. Predictor-lag combinations with a mean spatial correlation of >0.4 were kept for the next stage.

The remaining predictors were evaluated with principal component analysis and partial correlation analysis to eliminate any strongly covarying predictors (Figure 15). Manual backward elimination was used to simplify the models so that none contained more than five predictor variables. Variables were removed in a stepwise fashion to test whether their removal caused a significant drop in the r^2 value across a dozen random grid points.

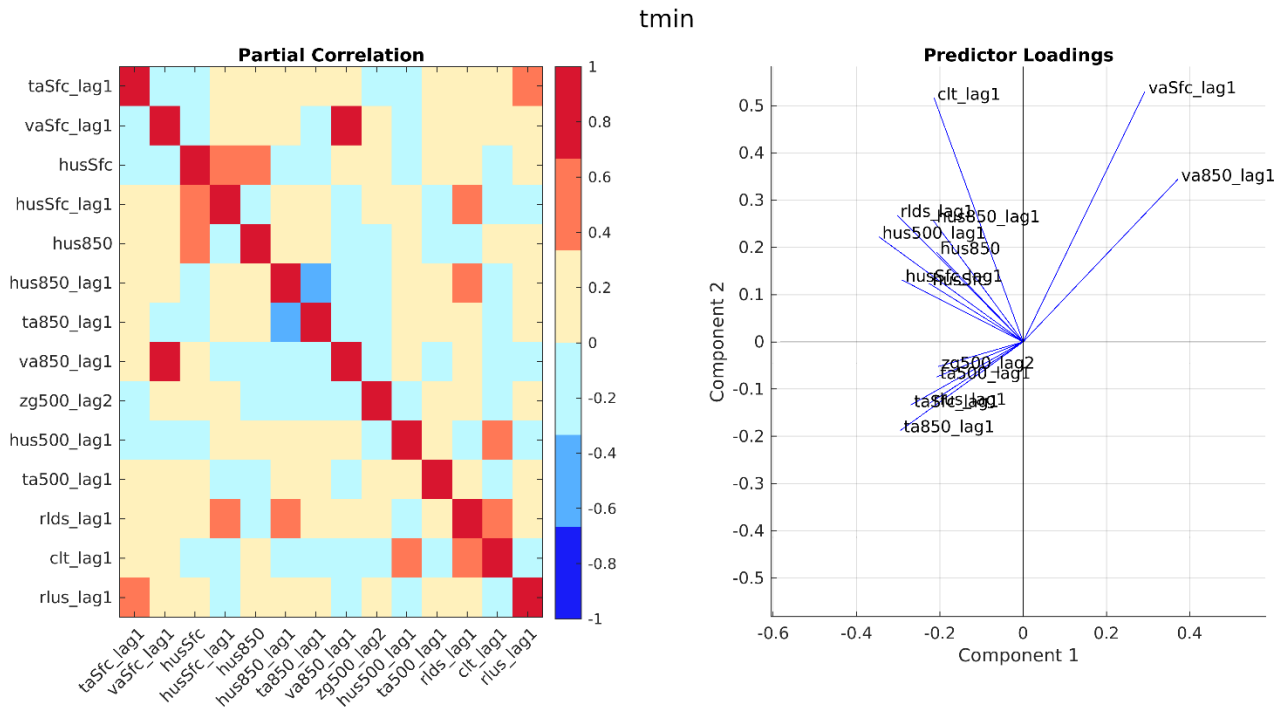

Figure 14. Example of predictor partial correlations and predictor loadings used to guide manual elimination as applied to minimum temperature. Partial correlation matrix of predictors is left. The first and second principal components of the predictors are plotted (right). These methods were used to help identify strongly covarying predictors and eliminate redundancy.

For the pre-screening of rainfall occurrence predictors, reanalysis lag-predictor combinations were divided into wet and dry groups according to local precipitation at each observation grid point. Statistical tests were then performed to select predictors of reanalysis data with discrete distributions in the wet and dry day groups. Due to the large sample size, a two sample Kolmogorov-Smirnov test was too sensitive (all predictors showed discrete continuous populations between wet and dry day groups), as was the Wilcoxon rank sum test (all predictors showed discrete medians in wet and dry day populations) and therefore unsuitable for eliminating predictors. Instead, an elimination criterion was developed whereby the predictor was retained if the median of both populations fell outside the interquartile range of the other.

Table 3. Final candidate predictors used in the GLM calibration.

tmin	tmax	vp	rad	rain-occurrence	rain- amount
taSfc_lag1	hurSfc	hurSfc	hurSfc	hurSfc_lag1	hus850_lag1
hus850	taSfc	va850_lag1	rsds	rsds	rsds_lag1
va850_lag1	rlus	rlds	clt_lag1	hus500_lag1	clt_lag1
clt_lag1		rsds		clt_lag1	pr_lag1
				va500_lag2	
				7-day Prob Precip	

Generalised Linear Model Calibration and Validation

A GLM is a form of multiple regression that uses the probability distribution of daily climate observations to fit a predictive model, where the observations are assumed to be drawn from the same distribution function family (for example, normal or gamma) (Yan et al., 2002). GLMs have been previously used for statistical downscaling and have been found to perform well (see, for example, Chandler et al., 2005, Asong et al., 2016, Beecham et al., 2014, Frost et al., 2011).

In this study, the GLM is used to downscale normally distributed variables (minimum and maximum temperature, radiation, and vapour pressure) using a Gaussian distribution and an identity link function. This is equivalent to a multiple linear regression equation.

Rainfall is modelled as a two-stage process in which the first stage (occurrence) uses the logistic regression form of a GLM. The sequence of wet and dry days in the predictand can be represented in binary form so that it has a binomial distribution, and the monotonic function is of the logit form.

The threshold for the probability of a predicted value is set as 0.5 such that days with a predicted probability of less than 0.5 were marked by a zero or non-occurrence (dry day), and days with a predicted probability greater than or equal to 0.5 were marked by a one or occurrence (wet day).

For the second stage, the mean amount of rainfall on a wet day is modelled as conditional on the predictor assuming a gamma distribution and a log link function.

For this study, GLM fitting was performed in a stepwise manner using the stepwiseglm function in the MATLAB Statistics and Machine Learning Toolbox (The Mathworks Inc., 2019). For all variables, the starting model specification was ‘constant’ and up to first-order interaction terms were permitted. A feature of climate processes is that there is commonly an inherent covariation between predictors, and including interactions allows these covariations to be represented as linear combinations of multiple predictors (Chandler and Wheater, 2002). The r^2 was used as a criterion for entry into the model with a threshold of 0.001 for entry and 0 for removal.

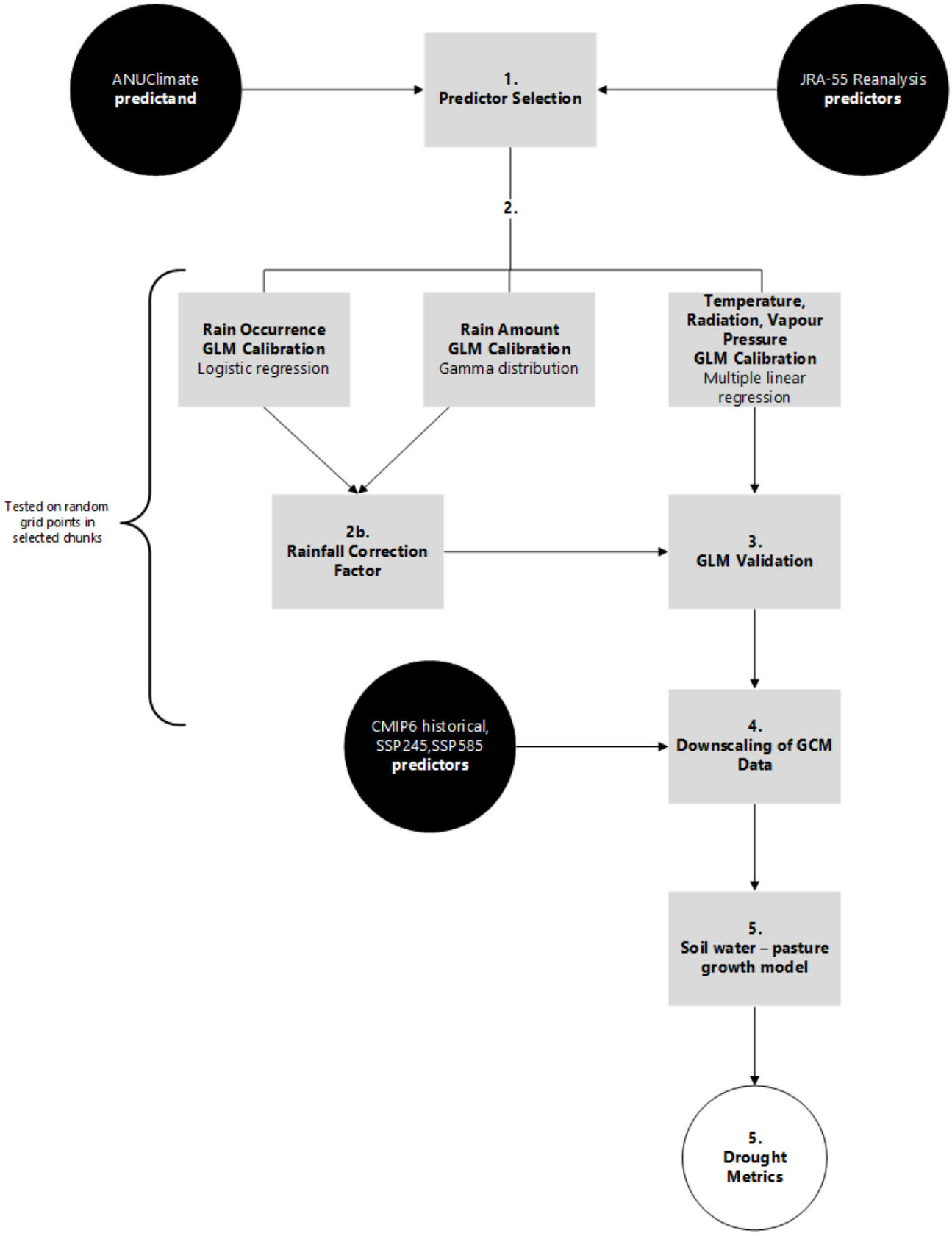

Figure 15. Detailed overview of the model calibration procedure for the ESD scheme.

Precipitation correction factor

After independent calibration of rainfall occurrence and amount (using the observed wet days), as part of the rainfall GLM calibration process, the amount model was rerun using the results of the occurrence model. This generates the modelled sequence of rainfall days using the calibration reanalysis data, in which a systematic underprediction of occurrence days and overprediction of mean rainfall was observed, caused by the heteroscedasticity inherent to rainfall observations. The underprediction of wet days is in contrast with the issues plaguing many GCMs, which suffer from a "drizzle effect" or too many wet days (Maraun et al., 2010; Fowler et al., 2007).

To correct for the over prediction of dry days and rainfall amount in the GLMs, a combined quantile mapping and frequency adaptation technique were used to generate a correction factor for each GLM. Prior to bias adjustment, it is necessary to determine a treatment for rainfall occurrences. This study uses the technique developed by Vrac et al. (2016) known as Singularity Stochastic Removal and similarly used in Cannon et al. (2015). Prior to bias adjustment, all values less than the wet day threshold (1 mm) in both the modelled and observed data are replaced with nonzero uniform random values. After bias adjustment, all data lower than the threshold are reset to 0, allowing both amount and occurrence to be corrected. The bias adjustment method used here is similar to the quantile mapping technique described by Cannon et al., (2015). The correction factor, CF, represents the quantile mapped difference between the cumulative distribution function (CDF) of the observed calibration rainfall (X_{oc}) and the CDF of the reanalysis modelled rainfall (X_{mc}) used in the GLM calibration.

$$CF = \frac{F_{oc}^{-1}(F_{mc})}{F_{mc}^{-1}(F_{mc})}$$

Eq. 1

where the numerator is the CDF of the reanalysis data evaluated at the quantiles of the observation data and the denominator is the CDF of the reanalysis modelled rainfall evaluated at the quantiles of the reanalysis modelled data, which simplifies to the modelled data, X_{mc}. The CF is stored for later use in the downscaling processing, during which the CF is multiplied with the data (X) to be corrected:

$$X_{corr} = CF * X$$

Eq. 2

In the calibration, X is the modelled rainfall based on reanalysis, and X_{corr} resolves to the observed rainfall. During downscaling processing, X is the modelled rainfall using GCM data for both historical and projection periods.

It should be noted that, unlike similar studies, this bias adjustment here is applied only to the bias in the GLMs and not to the GCM data. To distinguish between the other use of "bias correction" and its use here, we will refer to the bias-adjusted rainfall data as 'corrected', but not 'bias corrected.'

Model diagnostics

The performance of the GLM downscaled outputs were evaluated against the ANUClimate observations using multiple performance metrics: root mean square error (RMSE; Eq. 3), the mean bias (Bias; Eq. 4), the percent or relative bias (%Bias; Eq. 5), and the Pearson correlation coefficient (r; Eq. 5) as follows:

$$RMSE = \sqrt{\frac{1}{N}\sum_{i=1}^{N}(M_i - O_i)^2}$$

Eq. 3

$$BIAS = \frac{\sum_{i=1}^{N}(M_i - O_i)}{N}$$

Eq. 4

$$\%BIAS = \frac{\sum_{i=1}^{N}(M_i - O_i)}{\sum_{i=1}^{N} O_i} \times 100$$

Eq. 5

$$r = \frac{\sum_{i=1}^{N}(M_i - \overline{M})(O_i - \overline{O})}{(N-1)\sigma_M \sigma_O}$$

Eq. 6

Where M_i and O_i are the modelled and observed values, respectively, N is the number of paired observations, $\overline{M}$ and $\overline{O}$, and σ_M and σ_O are the averages and standard deviations of the respective datasets.

The metrics were calculated using the annual aggregations of the climate variables for the calibration and baseline periods. RMSE values range from 0 to +∞ and RMSE values closer to 0 indicate a higher model accuracy. BIAS values range from -∞ to +∞ and %BIAS values range from -100 to 100. BIAS and %BIAS values represent the under- or over-estimation of the model, and an optimal bias value is close to 0. The Pearson correlation coefficient (r) ranges from -1 to 1, where values closer to 1 indicate perfect positive correlation.

Results

Performance for climatology

Figure 17 shows the spatial distributions during the validation period (1996-2019) of the bias, relative bias, Pearson correlation coefficient and RMSE for the downscaled annually-averaged uncorrected and corrected rainfall, and minimum and maximum temperature.

Uncorrected rainfall shows a systematic negative bias to the observed rainfall and progressively higher RMSE from west to east. The northeast coast has RMSE values exceeding 400 mm/year. Correlation coefficients exceed 0.8 across most of the state with the Greater Sydney area showing the lowest correlation with observed data. There is substantial improvement in metrics for the corrected rainfall, with the bias becoming less systematic, and very low across most of the state. The correction factor appears to overcorrect along the North Coast, with a positive bias becoming evident after correction. There is also a slight reduction in r-values across much of the west likely due to the introduction of higher variance. There is however an improvement in the Sydney area. The RMSE improves considerably across the state (Table 4) in the corrected rainfall.

The GLM for minimum temperature has tendencies to underestimate temperature along the coast by up to 1°C, however there are strong correlations across the state ($r > 0.7$) (Table 3). RMSE tends to be less than 0.4°C other than in the northeast corner of the state and some other patchy areas. The GLM for maximum temperature performs extremely well with r-values greater than 0.9 across most of the state. Maximum temperature RMSE tends to be high in the south-west where the negative bias is up to 1°C.

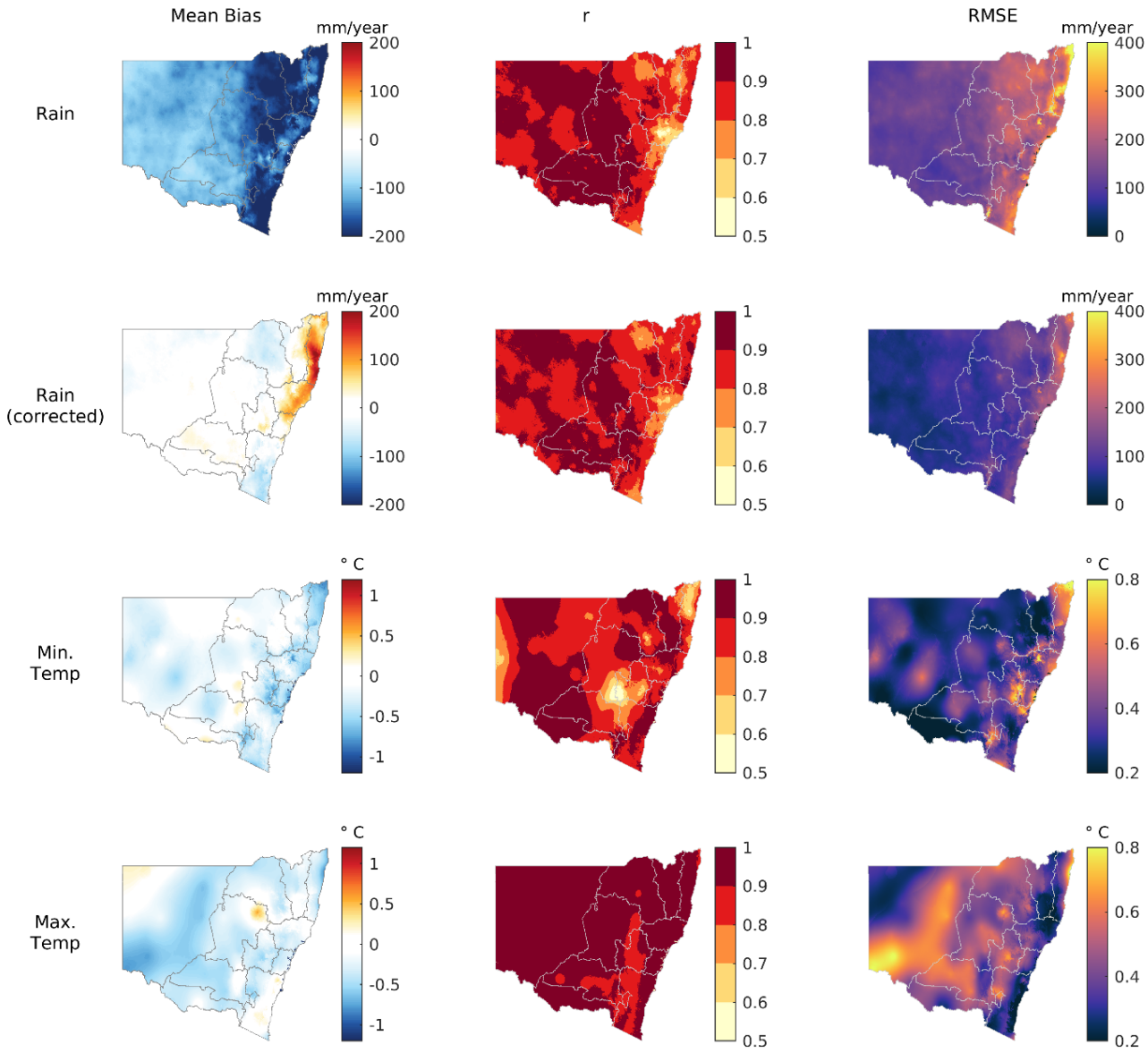

Figure 16. The bias, Pearson correlation coefficients (r), and the root mean square errors (RMSE) between the downscaled annual rainfall (uncorrected and corrected), minimum temperature and maximum temperature for the validation period (1996 – 2019). The correlation coefficients are significant at the 0.05 level.

Table 4. Spatially averaged statistical scores (Bias, % Bias, r, RMSE) of annual total rainfall and annual total corrected rainfall (mm/year) between the downscaled outputs and observations for the validation period (1996 -2019).

Local Land Services Region	Rainfall				Rainfall (corrected)			
	Bias	*% Bias*	*r*	*RMSE*	*Bias*	*% Bias*	*r*	*RMSE*
North Coast	-208.73	-16.43	0.82	283.29	105.59	8.51	0.87	207.02
Murray	-110.39	-25.48	0.92	124.26	8.39	2.11	0.91	71.26
Northern Tablelands	-196.21	-23.83	0.81	230.07	14.84	1.42	0.85	125.96
South East	-194.08	-26.43	0.87	211.37	-33.68	-4.72	0.87	104.40
Riverina	-103.07	-22.84	0.93	118.98	17.53	4.12	0.91	70.63
Central Tablelands	-164.81	-23.56	0.89	187.11	8.22	1.14	0.89	91.52
Hunter	-175.81	-20.72	0.75	217.89	57.32	6.08	0.79	144.30
Greater Sydney	-152.76	-17.52	0.78	188.14	29.17	3.25	0.78	124.51
Western	-105.50	-38.56	0.91	121.52	-8.46	-3.55	0.90	62.11
North West	-176.99	-30.85	0.86	200.46	-30.61	-5.45	0.85	113.10
Central West	-138.33	-27.16	0.92	156.00	21.71	3.51	0.91	170.20
NSW	-137.44	-30.32	0.89	159.12	3.53	-0.67	0.88	98.14

The GLM for minimum temperature has tendencies to underestimate temperature along the coast by up to 1°C, however there are strong correlations across the state ($r > 0.7$) (Table 5). RMSE tends to be less than 0.4°C other than in the northeast corner of the state and some other patchy areas. The GLM for maximum temperature performs extremely well with r-values greater than 0.9 across most of the state. Maximum temperature RMSE tends to be high in the south-west where the negative bias is up to 1°C.

Table 5. Spatially averaged statistical scores (Bias, % Bias, r, RMSE) of annual mean minimum and maximum temperature (°C) between the downscaled outputs and observations for the validation period (1996 -2019).

Local Land Services Region	Maximum Temperature				Minimum Temperature			
	Bias	*% Bias*	*r*	*RMSE*	*Bias*	*% Bias*	*r*	*RMSE*
North Coast	-0.33	-1.35	0.95	0.40	-0.50	-4.18	0.77	0.55
Murray	-0.32	-1.42	0.93	0.42	-0.05	-1.04	0.92	0.22
Northern Tablelands	-0.22	-0.96	0.95	0.34	-0.21	-2.4	0.89	0.31
South East	-0.10	-0.53	0.91	0.34	-0.31	-5.28	0.87	0.39
Riverina	-0.39	-1.67	0.91	0.52	-0.19	-2.11	0.88	0.33
Central Tablelands	-0.32	-1.54	0.90	0.49	-0.27	-3.73	0.76	0.43
Hunter	-0.18	-0.78	0.95	0.33	-0.37	-3.44	0.88	0.42
Greater Sydney	-0.29	-1.30	0.94	0.38	-0.48	-4.37	0.88	0.51
Western	-0.38	-1.43	0.95	0.50	-0.21	-1.65	0.88	0.31
North West	-0.26	-0.97	0.93	0.46	-0.12	-1.08	0.89	0.28
Central West	-0.21	-0.85	0.93	0.46	-0.16	-1.43	0.86	0.34
NSW	-0.30	-1.22	0.93	0.46	-0.22	-2.18	0.87	0.34

Performance for drought

The ability of downscaled climate ('model') variables to estimate drought is examined by calculating the relative bias from drought estimates derived from observations. This is performed from the 20th Century runs of the CMIP6 models for both PET methodologies (Figure 17). Relative bias is defined as the difference between the model and the observations normalised by the observations. It is expressed as a percentage difference. A negative relative bias means the model underestimates the observations, while a positive bias indicates an overestimation of the observations. Relative bias between the modelled and observed drought metrics was used to evaluate the performance of the downscaling method, weighting method, and individual GCMs. The individual GCM relative bias for the 10th percentile threshold drought metrics averaged over NSW for both PET methods is presented in Figure 17, with GCMs sorted from lowest to highest absolute value of relative bias.

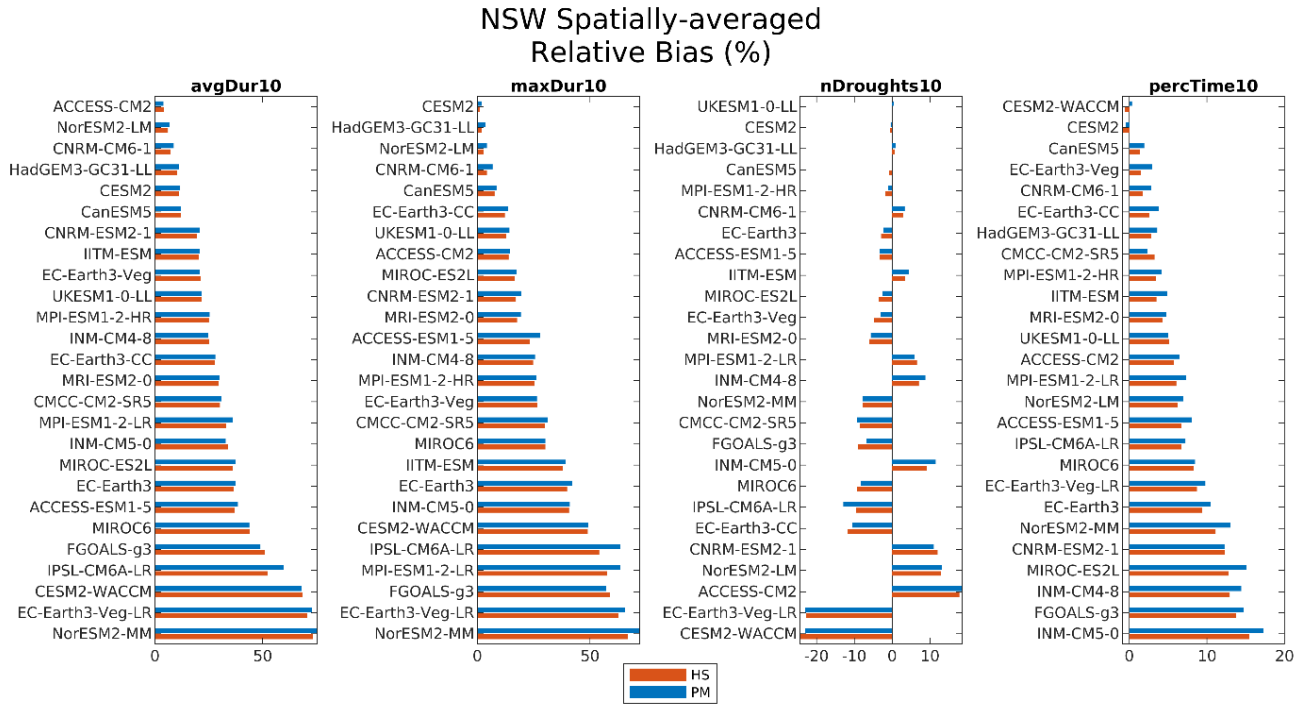

Figure 17. Spatially averaged relative bias for four drought metrics and 2 PET schemes at the 10th percentile threshold. avgDur10 is the average duration of drought, maxDur10 is the maximum drought duration, nDroughts10 is the number of droughts and percTime10 is the percentage of time spend in drought. HS is the Hargreaves-Samani PET method while PM is the Penman-Monteith method with constant wind run. GCMs are organised from least to greatest bias top to bottom for each drought metric.

At the 10th percentile threshold, most GCMs are overestimating metrics relating to the duration of drought (i.e., average and maximum duration, percent time) relative to the ANUClimate observations between 1995-2014. The biases range from 0 to ~60% for duration, and to about 20% for percent time. The frequency metric (number of droughts) shows a more normalised distribution of residuals, ranging from approximately -20 to 20% relative to observations. Generally, the Penman-Monteith PET-based metrics show a slightly larger bias than those calculated using Hargreaves-Samani, though these differences are relatively small for historical bias. Due to this result, subsequent summary plots will be shown using the HS results, however, results for PM are available and the implications for future projections are discussed in the main body of the report.

The bias found for a GCM is dependent on metric and there is limited consistency across the models (Figure 17). For example, ACCESS-CM2 performs well in capturing average duration but is ranked low for number of droughts and is in the middle range of the other two metrics. Similarly, CESM2-WACCM has the smallest bias for percent time and the highest for number of droughts. As previously shown in the skill weighting section, NorESM2-MM performs poorly across most metrics.

Implications for this study-GCM ensemble weighting scheme

The varied ability of the downscaling scheme to estimate observed climatology, as well as the downscaled CMIP6 ensemble to estimate observed properties of drought, requires careful consideration. Results range from encouraging where there appears to be acceptable biases and errors, to those where they would clearly lead to projections that have limited confidence.

The variability in bias across the GCM to reproduce the variable of interest (drought metrics) needs to be balanced against the use of 'model ensemble means' to build future projections. Ensemble approaches are used to aggregate model results and provide an estimate of the most likely future scenarios. Equally weighted multi-model means (or medians) are commonly used to evaluate ensemble results of projection studies as the ensemble mean is considered to be more representative than any single model. Recent studies have suggested using weighted ensembles that give more weight to models with higher skill and account for model independence (Sanderson et al., 2017, Knutti et al., 2017, Skahill et al., 2021). Subsequent ensemble results are shown using the skill-weighted ensemble mean.

In this study, we apply the skill and independence weight metric developed by Sanderson et al., (2017) to the ensemble using all the 10th percentile threshold metrics. The combined weighting method used here combines the relative skill of each model with a metric of independence, giving higher scores to less similar models and models with lower relative RMSE with the observations. To calculate the skill weight (Eq. 7), the RMSE between each GCM and observations for metrics of interest is calculated and normalized to the mean RMSE for that metric, such that the mean model has a value of 1, and GCMs with values less than one have relatively higher skill (Figure 18).

The combined RMSE matrix is used to calculate skill weight as follows:

$$w_{skill}(i) = e^{-\left(\frac{\delta_{i(obs)}}{D_q}\right)^2}$$

Eq. 7

where $\delta_{i(obs)}$ is the median of the normalized individual RMSEs for all metrics between each model i and the observations, and D_q is the radius of model quality, which determines the strength of the skill weighting (small values of D_q place more weight n models with higher skill). In this study, a value of 0.9 is used for D_q.

To calculate the independence score, an intermodel RMSE distance matrix is calculated for between all GCMs for a given metric and normalized by the mean RMSE for that metric. Higher intermodel distances are indicative of higher independence and lower similarity to other models. The mean inter-model distance, δ_{ij}, between models i and j for all metrics is used to calculate the similarity score $S(\delta_{ij})$:

$$S(\delta_{ij}) = e^{-\left(\frac{\delta_{ij}}{D_u}\right)^2}$$

Eq. 8

where Du is the radius of similarity, a parameter that specifies the distance scale for which the models' co-dependence is down-weighted. Du is calculated as the 1.5th percentile of δij, in this case, ~0.75. The final independence score, wind is calculated as the reciprocal of the sum of the similarities scores:

$$w_{ind}(i) = \left(1 + \sum_{i \neq j}^{n} S(\delta_{ij})\right)^{-1}$$

Eq. 9

where n is the total number of models.

Finally, the final GCM combined skill and independence weight (Table 6) is calculated using both the skill weight and independence weight normalized by a constant, A, such that the weights across all models sum to one:

$$w(i) = A w_{skill}(i) w_{ind}(i)$$

Eq. 10

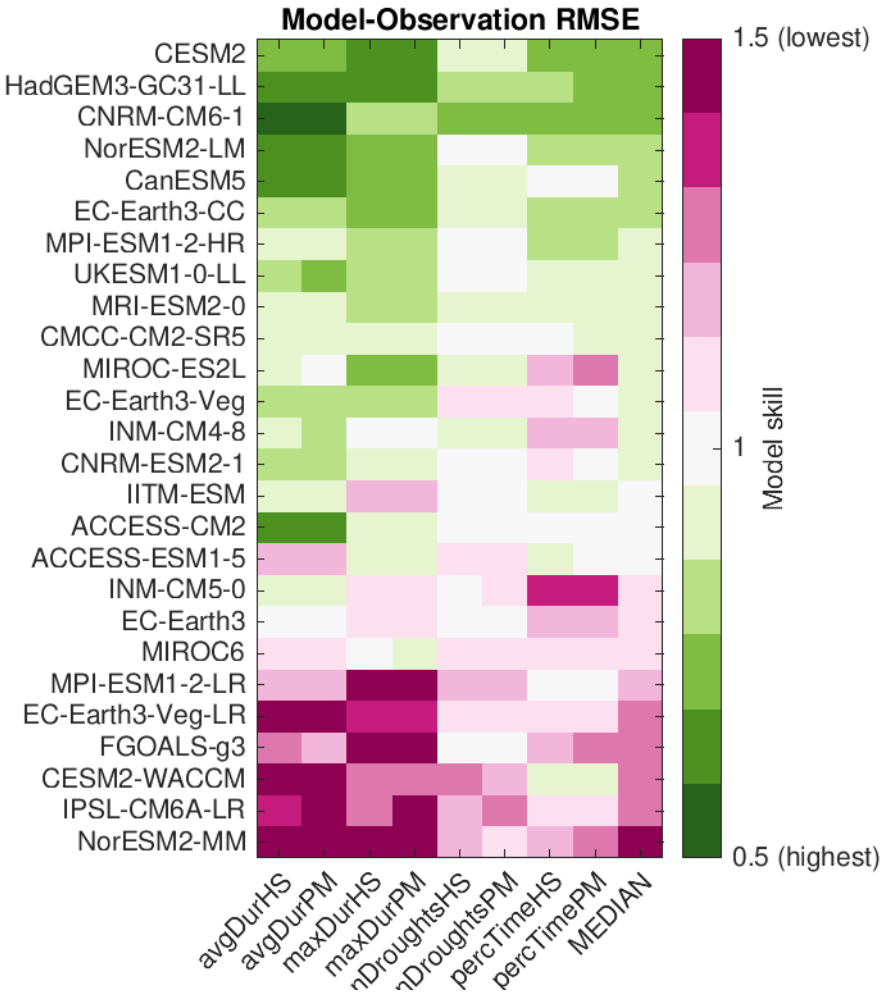

Figure 18. Model skill matrix for multiple drought metrics (columns) based on normalised RMSE. Values greater than 1 indicate models with poorer skill, and values less than 1 indicate models with higher skill. Models are sorted by the median skill across all metrics used for weighting (δi(obs); shown in the final column).

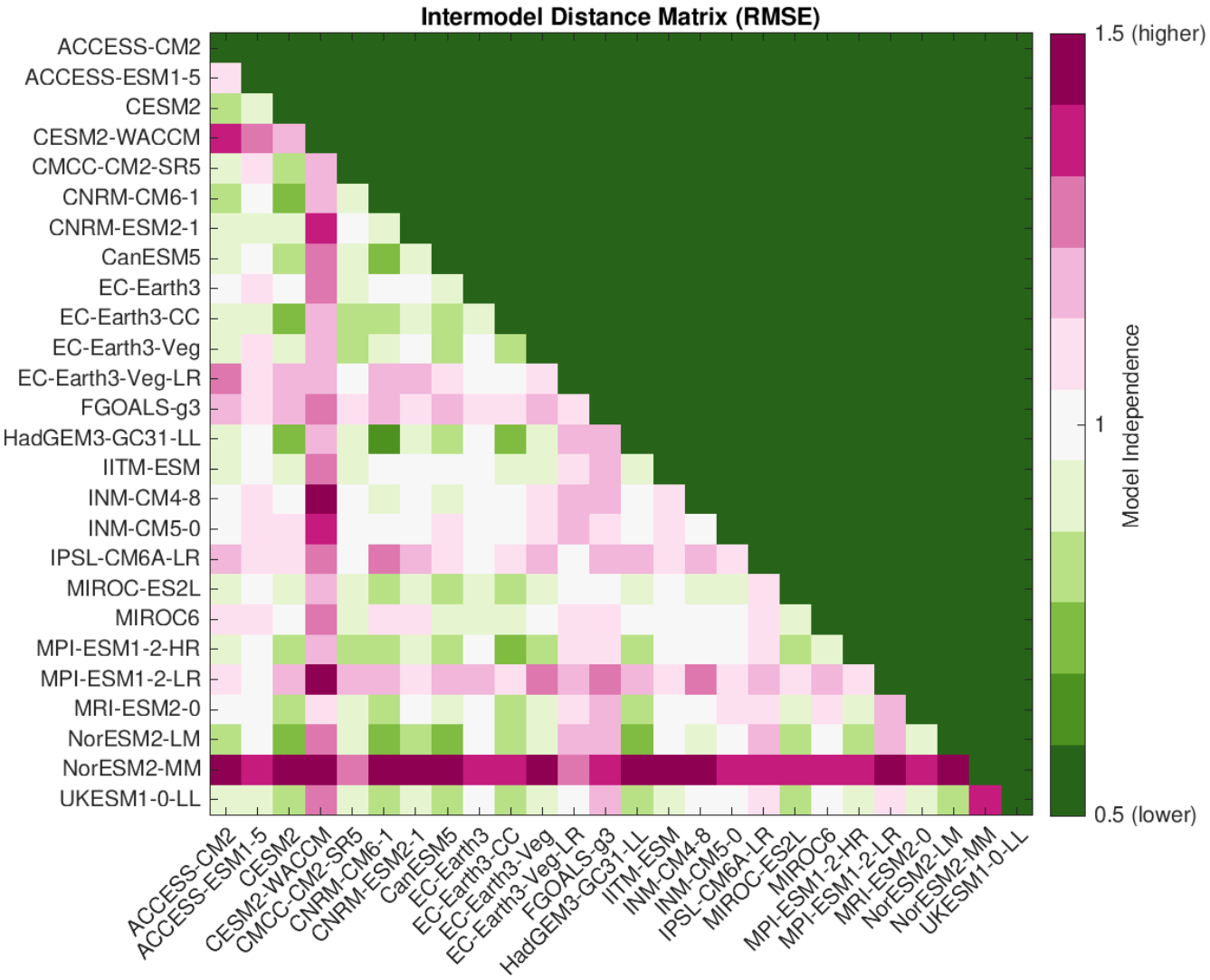

Figure 19. RMSE intermodel distance matrix used to quantify the independence scores. The intermodel distance matrix is calculated as the mean of the RMSE scores between models for each drought metric used in the skill scores, normalised to the mean of the matrix. Red colours (high values) indicate highly independent models while green colours (lower values) depict higher dependence or similarities.

Table 6. Independence, skill and combined weights for the multi-model ensemble. Models are sorted in descending order by combined weight.

CMIP6 Model	Ind. Weight	Skill Weight	Combined
CESM2	0.150	0.540	0.053
HadGEM3-GC31-LL	0.149	0.529	0.051
CNRM-CM6-1	0.150	0.502	0.049
INM-CM4-8	0.211	0.338	0.047
NorESM2-LM	0.153	0.467	0.046
CanESM5	0.154	0.458	0.046
MRI-ESM2-0	0.174	0.381	0.043
EC-Earth3-CC	0.141	0.449	0.041
CNRM-ESM2-1	0.186	0.337	0.041
MPI-ESM1-2-HR	0.158	0.395	0.041
IITM-ESM	0.194	0.319	0.040
EC-Earth3-Veg	0.177	0.348	0.040
UKESM1-0-LL	0.155	0.394	0.040
CMCC-CM2-SR5	0.166	0.366	0.039
ACCESS-ESM1-5	0.206	0.287	0.038
CESM2-WACCM	0.399	0.147	0.038
INM-CM5-0	0.221	0.252	0.036
MIROC-ES2L	0.157	0.353	0.036
MPI-ESM1-2-LR	0.307	0.176	0.035
ACCESS-CM2	0.178	0.302	0.035
EC-Earth3	0.195	0.249	0.032
MIROC6	0.200	0.232	0.030
FGOALS-g3	0.285	0.152	0.028
EC-Earth3-Veg-LR	0.263	0.156	0.027
IPSL-CM6A-LR	0.271	0.135	0.024
NorESM2-MM	0.557	0.062	0.023

Figure 20 shows the ensemble median and skill-weighted ensemble of the relative biases for the 10th percentile HS PET method. Though Figure 20 indicates spatially-averaged positive biases, there is actually substantial variation in the biases across the state. Negative biases in duration and percent time are observed in the central-west and south-east of the state. The use of the weighted ensemble reveals substantial reductions in the bias for all duration metrics. There is some increase in bias for number of droughts, but this increase is smaller in magnitude than the reduction gains achieved in duration. Therefore, the weighted ensemble is used for presenting future results.

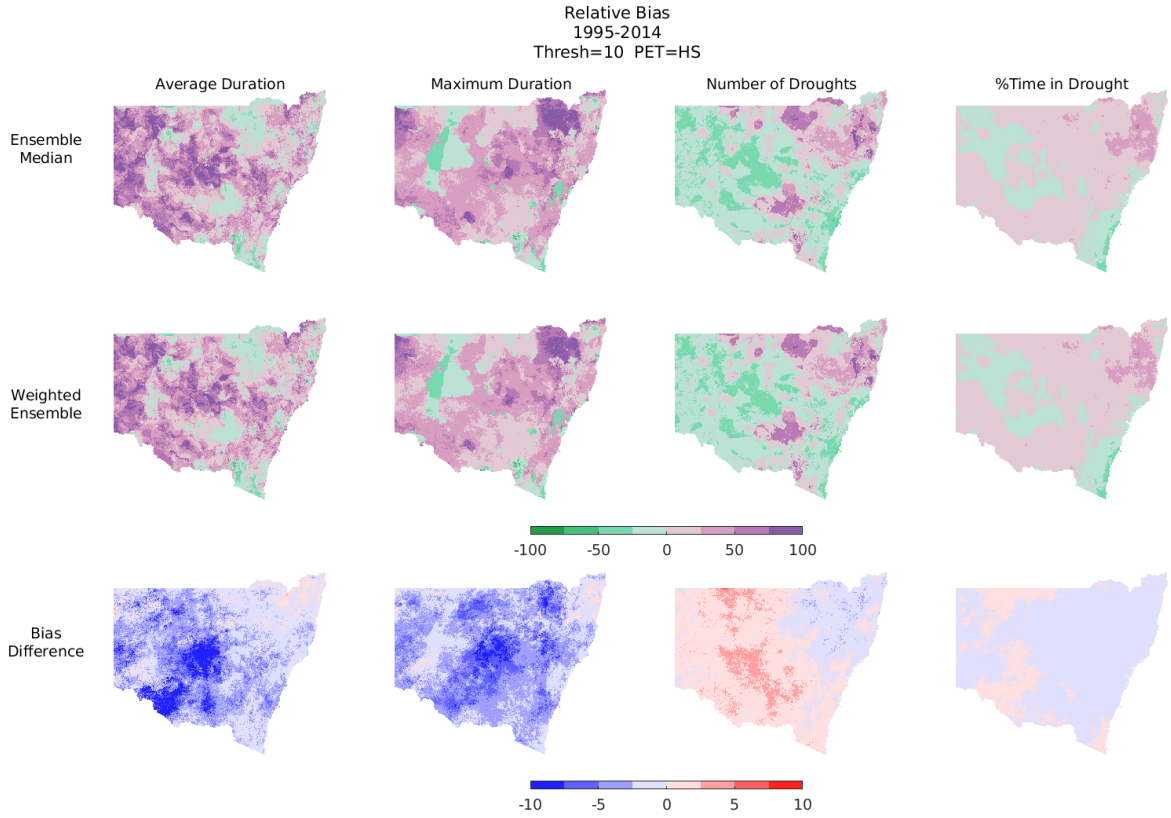

Figure 20. (first row) Multimodel median of relative bias for the 10th percentile threshold and HS PET (unweighted); (second row) Ensemble using skill-based weighting; (third row) The difference between the weighted ensemble bias and the ensemble median bias. Blue values indicate a reduction in the overall relative bias of the ensemble.

Appendix 2. Evapotranspiration methodology

Background

Evapotranspiration is an important flux process to account for when developing future scenarios of drought, and this section is concerned with selecting an appropriate methodology for this study. Along with precipitation, it is a major component of the hydrological cycle. Evapotranspiration, the exchange of water from the earth's surface to the lower atmosphere, influences the intensity and duration of a drought as well as the timing of entry and recovery. The rate of evapotranspiration is determined by the ambient climate, principally radiation and temperature, with secondary factors like wind and vapor pressure also affecting the process. Surface properties, including albedo and vegetation condition, also modify the rate of exchange.

The regulation of evapotranspiration by temperature links drought risk to the warming trends evident under anthropogenic climate change. It is common to assume that future droughts will increase in intensity as temperatures rise. However, the strength of this assumption is the subject of physical and methodological debate. For example, the radiation budget or latent heat (energy) required for evaporation at differing air temperatures is affected by cloud and may dampen the average rate of evapotranspiration as the atmosphere becomes more tropical in a warmer climate. This type of regulation of the evapotranspiration process and the strength of feedback is regionally specific, given latitude effects on seasonal radiation and shifts in future tropical convection.

There are also methodological factors in the calculation of evapotranspiration rates which can influence drought determination (Box 1 provides some examples of the main technical approaches). Simple empirical temperature or radiation driven approaches could create biases because they don't include key feedbacks, like the effects of humidity on vapour pressure and are overly sensitive to temperature trends. More physically based and complex approaches like the Penman-Monteith equation include factors like wind, which then brings in limitations around the quality of forcing data. Most approaches do not capture the full suite of dynamic feedbacks between vegetation and the lower atmosphere through the evapotranspiration process, which requires the use of a fully coupled land-atmosphere-ocean model. Evapotranspiration is also difficult to measure in the field, and there is only a limited observational network to validate different approaches across NSW.

The system used to quantify drought in this study (EDIS and DPI AgriMod) adopts the common approach of calculating potential evapotranspiration (PET). PET is the demand

for water by the lower atmosphere at the standard assumed boundary layer of crop/pasture canopy, a height of 1.5m from the earth's surface. Here:

- PET is derived from constituent standardised climatic variables (for example, rainfall, temperature) and used as an input to the AgriMod soil water balance where actual evapotranspiration (AET) is determined.
- no partitioning between bare soil (evaporation) and stomatal conductance of water (transpiration) is made in the model, although AET is regulated by pasture and crop vigour.

While this approach has merit and is well validated, it is relatively simple. It does not encapsulate the full set of dynamic feedback processes between crops, pastures and the lower atmosphere that may occur under a warmer, more carbon dioxide enriched environment. There are also different methodologies available to calculate PET which could affect drought determination. Given this limitation and to build a practical methodology, the approach taken in this study has been to:

- proceed with the construction of future drought scenarios with full knowledge of the limitations of the EDIS system.
- to aid the interpretation of the regional drought scenarios, develop more detailed knowledge of the implications of different PET determination methods by undertaking some exploratory analysis.

Box 1- Examples of the general types of evapotranspiration models

Mechanistic

The FAO's derivation of the Penman-Monteith equation (Monteith and Unsworth 1990, Allen et al., 1998) is a reference mechanistic approach because it is based on a full range of processes influencing transfer of water to the atmosphere, including resistance from soil and plants. An example FAO-56 (Doorenbos and Pruit, 1977 version of the Penman-Monteith equation is:

$$E_p = \frac{\Delta(R_n - G_s) + 86.4\rho c_p \delta / r_a}{\lambda(\Delta + \gamma)}$$

where E_p is potential soil evaporation, Δ is the slope of the saturated vapour pressure deficit curve (kPa $°C^{-1}$), R_n is the net radiation (MJ m^{-2} d^{-1}), G_s is the soil heat flux (MJ m^{-2} d^{-1}), ρ is the air density (kg m^{-3}) C_p the specific heat of the air (kJ kg^{-1} $°C^{-1}$) and δ the vapour pressure deficit (kPa), ra the aerodynamic resistance (s m^{-1}), λ the latent heat of vaporization (MJ kg^{-1}) and γ is the psychometric constant (kPa $°C^{-1}$).

Conceptual

There are also simpler algorithms based on partial representations of processes, such as Priestly-Taylor, Blaney-Criddle and Hargreaves-Samani Ep (Allen et al., 1998). The radiation-based Priestly-Taylor equation is reproduced here as an example. It calculates E_p as a function of the latent heat of vaporization and the heat flux in a water body:

$$E_p = \alpha\left(\frac{s}{s+\lambda}\right)\left(\frac{(Q_a - Q_x)}{L}\right)$$

where α is an empirically defined constant, *s* is the slope of the saturated pressure temperature gradient, λ is the psychometric constant, Q_x is the change in heat stored in a water body (MJ/m^2/day), L is the latent heat of vaporization (MJ/kg) and Qn is the net radiation supplied as an independent variable (MJ/m^2/day).

Empirical

It is also possible to model evapotranspiration empirically. For example, Xu and Singh (2002) derived a modified form of the Blaney-Criddle algorithm:

$$Ep = (\lambda R)(T + \beta)$$

where R is incoming shortwave solar radiation, and T is the mean air temperature (°C/week). The parameters λ and β are constants obtained by calibration and the equation is known to exhibit moderate to high accuracy when well calibrated (Xu and Singh, 2002).

Exploratory analysis

Evaporation models for NSW

As a step towards building an informed approach to the methodology for determining PET in this study some exploratory analysis was undertaken, initially looking at different forms for calculation, their sensitivity to different climate forcing and implications for determination of drought. In this study one conceptual and two form of mechanistic PET models are trailed:

- the Conceptual Hargreaves-Samani model (HS).
- the mechanistic Penman-Monteith equation where wind is held constant (PM-C).

- the mechanistic Penman-Monteith equation where wind data is obtained from a separate historical experimental data set provided by the CSIRO (PM-W).

Using observation data (ANUClimate) as forcing variables, Figure 22 plots the average annual evaporation derived from a conceptual (HS) and the two mechanistic models. The fourth representation are PET observation, interpolated from the sparse (<30 site) class A Pan network. All the plots are broadly similar in that they capture the east to west gradient in annual PET across NSW. The magnitude of the flux is comparatively higher in western NSW in the observation data. There are fine, subtle regional differences in the rates of different PET models. The rate of annual average PET changes in the coastal hinterland of northern NSW, for example, depends on whether observed or constant wind is used in the Penman Monteith equation.

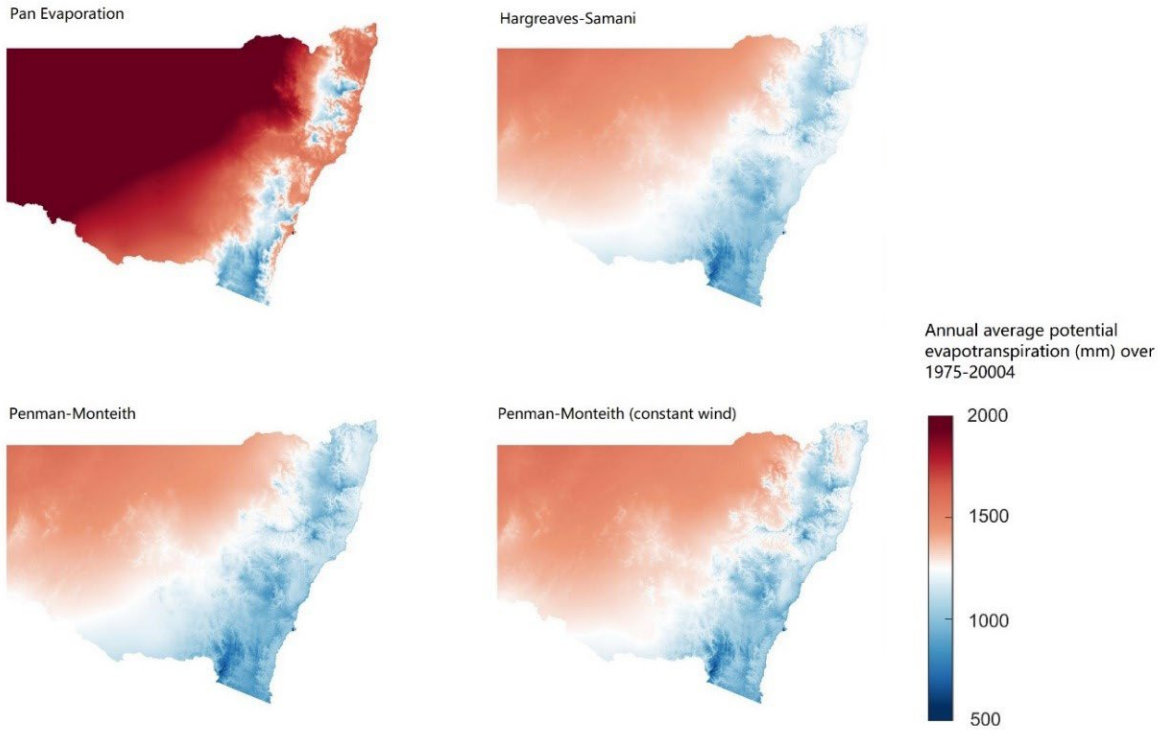

Figure 21. Annual average potential evaporation comparison analysis for 1975 to 2004 for pan evaporation; Hargreaves-Samani method; FAO56 Penman-Monteith method; and FAO56 Penman Monteith with constant wind method.

Sensitivity of evaporation to climate forcing

To better understand the baseline processes forcing PET fluxes across NSW, the sensitivity of class A Pan observations to changes in different climate variables was assessed (Figure 22). This is based on the methodology described by McCuen et al. (1974). The closer the sensitivity metric in Figure 22 is to a value of 1 the stronger the relative contribution of the forcing variable is to the PET flux. The results in Figure 22 suggest that the regional distribution of radiation forcing is relatively uniform across

regional NSW. There are dramatic differences in the sensitivity of PET to shifts in maximum temperature between regions, while minimum temperature has a relatively small effect on PET in NSW. Similarly, vapour pressure (vp) and the vapour pressure deficit (vpd) have pronounced regional differences.

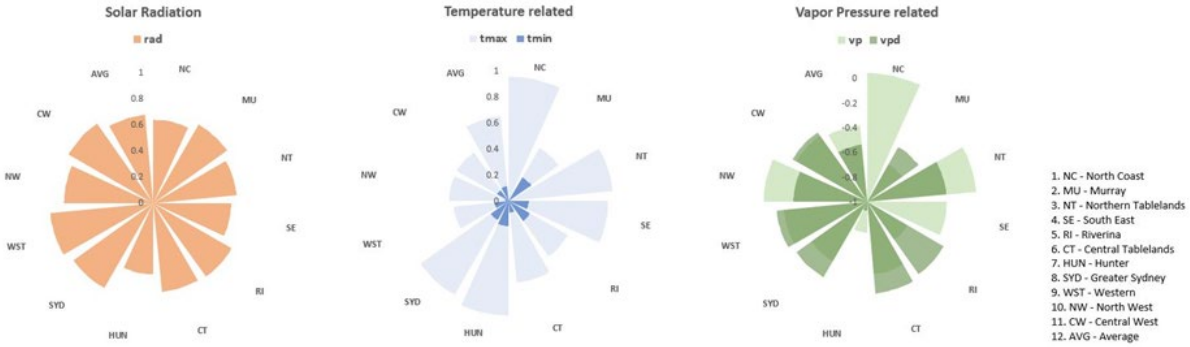

Figure 22. Local Land Services Region distribution of the sensitivity of mean annual potential evaporation (PET) to changes in climate forcing (solar radiation, temperature and vapor pressure).

The sensitivity analysis methodology devised by McCuen et al., (1974) was the adapted to examine the relative contribution of forcing on PET for the HS and PM-W equations in both drought and non-drought periods (Table 7). The analysis highlights that the amplifying effect of radiation and maximum temperature on PET are amplified during drought periods, and the dampening effect of VP is similarly increased during a drought. These effects are greater in magnitude when utilising the PM-W determination of PET. Wind, in the framework of PM-W, amplifies PET during droughts and dampens the flux in non-drought years.

Table 7. PET sensitivity to climate forcing in drought and non drought years (1975-2020). Data are aggregated across NSW.

Drought Period	rad		T_{max}		T_{min}		vp		vpd		wind speed	
	HS	*PM-W*	*HS*	*PM-W*	*HS*	*PM-W*	*HS*	*PM-W*	*HS*	*PM-W*	*HS*	*PM-W*
Non-drought*	0.380	0.784	0.526	0.555	0.045	0.049	-0.276	-0.393	-0.622	-0.701	0.031	-0.262
Drought+	0.435	0.900	0.597	0.726	0.100	0.215	-0.352	-0.589	-0.531	-0.586	-0.035	0.226

*Non-drought years are 1976-1982, 1985-1995, and 2011-2016. +Drought years are 1996-2010 and 2017-2022

Evaporation and drought characterisation

To evaluate the implications of using differing PET methodologies on the characterisation of drought in NSW, the EDIS system was re-run from 1975-2020 using the HS and the PM-W methodology. To undertake the analysis, the CDI was converted into a continuous rather than categorical metric by taking the minimum of the three indices, described as the Minimum Drought Index or MDI for clarity.

The scatter plots in Figure 23 show the relationship between the two methods across NSW, where colour coding is used to show the strength of the correlation for individual data points. Generally, there is a strong positive correlation between the methods, indicating that there is limited effect on PET on the value of drought indicators across their full range. Close inspection of the data also reveals that the correlations do weaken in some ranges of drought indicators, particularly in the range that is close to or below the value that would signify a drought event (the 5th-30th percentile). This suggests that drought determination in most of NSW is not overtly sensitive to PET methodology selection, but there are sub regions where it will be influential. Importantly in this small number of cases, the HS method would overestimate drought in comparison to the PM-W method.

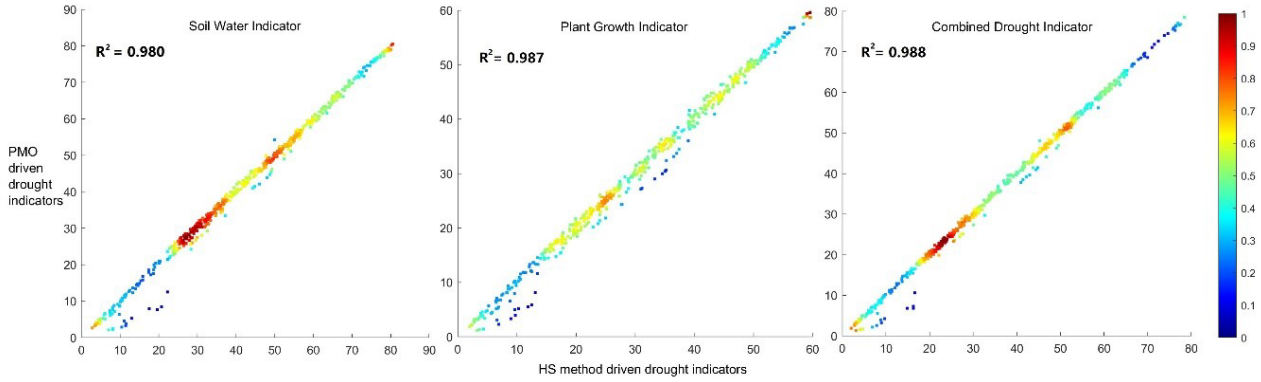

Figure 23. Scatter density plot between Hargreaves-Samani (HS) and Penman-Monteith (PMO using the PM-C method) driven monthly drought indicators in NSW from 1975 – 2020. Each data point in space represents the spatial average of the PET-driven indicator. The Soil Water Indicator, Plant growth Indicator and Combined Drought Indicator are from the EDIS system. The colours represent the correlation coefficient between the PET-indicators of individual data points in the NSW domain.

This pattern of results is explored further by closely examining how the two methodologies would have determined the 2017-2020 drought sequence (Figure 24). The MDI time series (c) highlights strong agreement during the drought onset and extension period in 2016 through to 2019. Differences begin to emerge in terms of the rate of drought recovery window where the amplifying effect of maximum temperature on the ETo rate from the maximum temperature in the PM-W method would lengthen the drought window. Figure 24 (a and b) are spatial plots of the mean MDI during the full drought sequence. While structurally similar, there are some small sub regional differences if the data is inspected closely.

Based on this analysis, the differing PET methodologies on the historical period presented in this section they appear to be broadly similar, and there would be little difference between them in terms of state-wide drought determination at a large scale. However, sub-regional differences are evident and need to be considered for land holders in those regions where they may be greater exposure to shifts in temperature and vapour pressure. The pragmatic choice for this study at this point is to utilise the Hargreaves-Samani methodology, simply because it negates the need to utilise wind

data where there are significant quality deficiencies in Australia's daily observation as well as the concerns about modelled wind-run projections. However, because the analysis is undertaken in the historical window, there may be further non-stationarity effects that also need to be identified. The choice of PET methodology is revisited in the section on downscaling and reported in the section describing NSW Drought scenarios.

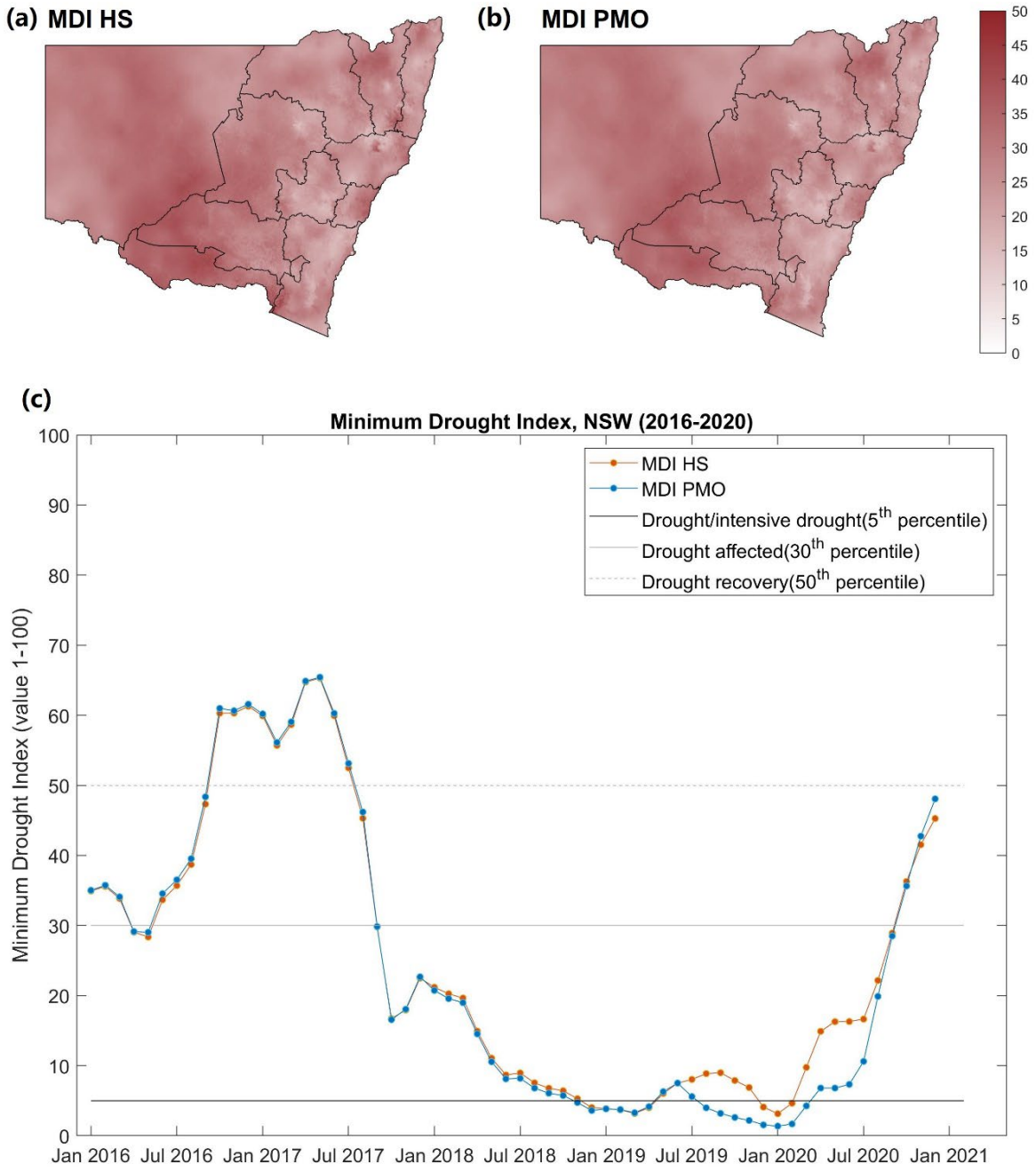

Figure 24. The influence of potential evaporation method on the characterisation of 2017-2020 drought across NSW. (a) map of the average MDI (2016-2021) using the Hargreaves-Samani (HS) PET method. (b) map of the average MDI (2016-2021) using the Penman-Monteith with fill wind (PM-W) PET method. (c) The time series of spatially averaged MDI for NSW using both the HS (red) and PMO-C (blue) methods.

References

Allen, R.G., Pereira, L.S., Raes, D., Smith, M., 1998. Crop evapotranspiration - Guidelines for computing crop water requirements - FAO Irrigation and drainage paper 56 15.

Asong, Z.E., Khaliq, M.N., Wheater, H.S., 2016. Multisite multivariate modeling of daily precipitation and temperature in the Canadian Prairie Provinces using generalized linear models. Clim Dyn 47, 2901–2921. https://doi.org/10.1007/s00382-016-3004-z

Beecham, S., Rashid, M., Chowdhury, R.K., 2014. Statistical downscaling of multi-site daily rainfall in a South Australian catchment using a Generalized Linear Model. International Journal of Climatology 34, 3654–3670. https://doi.org/10.1002/joc.3933

Benestad, R. E., 2001. A comparison between two empirical downscaling strategies. Int. J. Climatol., 21, 1645–1668.

Benestad, R.E., Chen, D., Hanssen-bauer, I., 2008. Empirical-statistical Downscaling. World Scientific Publishing Company.

Cannon, A.J., Sobie, S.R., Murdock, T.Q., 2015. Bias Correction of GCM Precipitation by Quantile Mapping: How Well Do Methods Preserve Changes in Quantiles and Extremes? Journal of Climate 28, 6938–6959. https://doi.org/10.1175/JCLI-D-14-00754.1

Chandler, R.E., Wheater, H.S., 2002. Analysis of rainfall variability using generalized linear models: A case study from the west of Ireland. Water Resources Research 38, 10-1-10–11. https://doi.org/10.1029/2001WR000906

Clark, A., Mullan, B., Porteous, A., 2011. Scenarios of regional drought under climate change. National Institute of Water & Atmospheric Research.

Clark, D.A., Wurtzel, D.J., Zhu, D.E.Q., Broadfoot, K., Wallace, S., 2019. Drought in a Changing Climate. NSW Climate Change Strategy for Primary Industries Vulnerability Assessment Special Report on Drought.

CSIRO and Bureau of Meteorology, 2015. Climate change in Australia information for Australia's natural resource management regions: technical report.

Dai, A., 2011. Drought under global warming: a review. WIREs Climate Change 2, 45–65. https://doi.org/10.1002/wcc.81

DAWE, 2021. Farm Management Deposits Scheme: 2021 evaluation. Department of Agriculture, Water and the Environment, Canberra, CC BY 4.0.

DAWE, 2022. Future Drought Fund Annual Report 2021-22. Department of Agriculture, Water and the Environment, Canberra, CC BY 4.0.

Donohue, R.J., Hume, I.H., Roderick, M.L., McVicar, T.R., Beringer, J., Hutley, L.B., Gallant, J.C., Austin, J.M., van Gorsel, E., Cleverly, J.R., Meyer, W.S., Arndt, S.K., 2014. Evaluation of the remote-sensing-based DIFFUSE model for estimating photosynthesis of vegetation. Remote Sensing of Environment 155, 349–365. https://doi.org/10.1016/j.rse.2014.09.007

Doorenbos, J. and Pruit, W.O., 1977. Crop Water Requirements, FAO Irrigation and Drainage and Paper No 24. Food and Agriculture Organization.

Evans, J.P., Ji, F., Lee, C., Smith, P., Argüeso, D., Fita, L., 2014. Design of a regional climate modelling projection ensemble experiment – NARCliM. Geosci. Model Dev. 7, 621–629. https://doi.org/10.5194/gmd-7-621-2014.

Fowler, H.J., Ekström, M., Blenkinsop, S., Smith, A.P., 2007. Estimating change in extreme European precipitation using a multimodel ensemble. Journal of Geophysical Research: Atmospheres 112. https://doi.org/10.1029/2007JD008619

Frost, A.J., Charles, S.P., Timbal, B., Chiew, F.H.S., Mehrotra, R., Nguyen, K.C., Chandler, R.E., McGregor, J.L., Fu, G., Kirono, D.G.C., Fernandez, E., Kent, D.M., 2011. A comparison of multi-site daily rainfall downscaling techniques under Australian conditions. Journal of Hydrology 408, 1–18. https://doi.org/10.1016/j.jhydrol.2011.06.021

Gallant, A.J., Reeder, M.J., Risbey, J.S., Hennessy, K.J., 2013. The characteristics of seasonal-scale droughts in Australia, 1911–2009. International Journal of Climatology 33, 1658–1672.

Gibbs, W.J., Maher, 1967. Rainfall deciles as drought indicators.

Hennessy, K., Lucas, C., Nicholls, N., Bathols, J., Suppiah, R., Ricketts, J., 2005. Climate change impacts on fire-weather in south-east Australia. Climate Impacts Group, CSIRO Atmospheric Research and the Australian Government Bureau of Meteorology, Aspendale.

Holzworth, D.P., Huth, N.I., deVoil, P.G., Zurcher, E.J., Herrmann, N.I., McLean, G., Chenu, K., van Oosterom, E.J., Snow, V., Murphy, C., Moore, A.D., Brown, H., Whish, J.P.M., Verrall, S., Fainges, J., Bell, L.W., Peake, A.S., Poulton, P.L., Hochman, Z., Thorburn, P.J., Gaydon, D.S., Dalgliesh, N.P., Rodriguez, D., Cox, H., Chapman, S., Doherty, A., Teixeira, E., Sharp, J., Cichota, R., Vogeler, I., Li, F.Y., Wang, E., Hammer, G.L., Robertson, M.J., Dimes, J.P., Whitbread, A.M., Hunt, J., van Rees, H., McClelland, T., Carberry, P.S., Hargreaves, J.N.G., MacLeod, N., McDonald, C., Harsdorf, J., Wedgwood, S., Keating, B.A., 2014. APSIM – Evolution towards a new generation of agricultural systems simulation. Environmental Modelling & Software 62, 327–350. https://doi.org/10.1016/j.envsoft.2014.07.009

Kirono, D.G.C., Round, V., Heady, C., Chiew, F.H.S., Osbrough, S., 2020. Drought projections for Australia: Updated results and analysis of model simulations. Weather and Climate Extremes 30, 100280. https://doi.org/10.1016/j.wace.2020.100280

Kirschbaum, M.U.F., Rutledge, S., Kuijper, I.A., Mudge, P.L., Puche, N., Wall, A.M., Roach, C.G., Schipper, L.A., Campbell, D.I., 2015. Modelling carbon and water exchange of a grazed pasture in New Zealand constrained by eddy covariance measurements. Science of The Total Environment 512–513, 273–286. https://doi.org/10.1016/j.scitotenv.2015.01.045

Knutti, R., Sedláček, J., Sanderson, B.M., Lorenz, R., Fischer, E.M., Eyring, V., 2017. A climate model projection weighting scheme accounting for performance and interdependence. Geophysical Research Letters 44, 1909–1918. https://doi.org/10.1002/2016GL072012

Maraun, D., Wetterhall, F., Ireson, A.M., Chandler, R.E., Kendon, E.J., Widmann, M., Brienen, S., Rust, H.W., Sauter, T., Themeßl, M., Venema, V.K.C., Chun, K.P., Goodess, C.M., Jones, R.G., Onof, C., Vrac, M., Thiele-Eich, I., 2010. Precipitation downscaling under climate change: Recent developments to bridge the gap between dynamical models and the end user. Reviews of Geophysics 48. https://doi.org/10.1029/2009RG000314

McCuen, R.H., 1974. A sensitivity and error analysis CF procedures used for estimating evaporation 1. JAWRA Journal of the American Water Resources Association 10, 486–497.

Monteith, J., Unsworth, M., 1990. Principles of Environmental Physics. (2nd edn.) Edward Arnold.

Mpelasoka, F., Hennessy, K., Jones, R., Bates, B., 2008. Comparison of suitable drought indices for climate change impacts assessment over Australia towards resource management. International Journal of Climatology 28, 1283–1292. https://doi.org/10.1002/joc.1649

Murphy, B.F., Timbal, B., 2008. A review of recent climate variability and climate change in southeastern Australia. International Journal of Climatology 28, 859–879. https://doi.org/10.1002/joc.1627

Nicholls, N., 2004. The Changing Nature of Australian Droughts. Climatic Change 63, 323–336. https://doi.org/10.1023/B:CLIM.0000018515.46344.6d

Nix, H.A., 1981. Simplified simulation models based on specified minimum data sets: the CROPEVAL concept.

O'Neill, B.C., Tebaldi, C., van Vuuren, D.P., Eyring, V., Friedlingstein, P., Hurtt, G., Knutti, R., Kriegler, E., Lamarque, J.-F., Lowe, J., Meehl, G.A., Moss, R., Riahi, K., Sanderson, B.M., 2016. The Scenario Model Intercomparison Project (ScenarioMIP) for CMIP6. Geoscientific Model Development 9, 3461–3482. https://doi.org/10.5194/gmd-9-3461-2016

Pulwarty, R.S., AND. Sivakumar, M.V.K., 2014. Information systems in a changing climate: Early warnings and drought risk management, Weather and Climate Extremes,3,14-21.

Regional NSW 2022. Drought Measures- Strategic Evaluation, September 2022, State of NSW through Regional NSW.

Sanderson, B.M., Wehner, M., Knutti, R., 2017. Skill and independence weighting for multi-model assessments. Geoscientific Model Development 10, 2379–2395. https://doi.org/10.5194/gmd-10-2379-2017

Seneviratne, S.I., 2012. Historical drought trends revisited. Nature 491, 338–339. https://doi.org/10.1038/491338a

Sepulcre-Canto, G., Horion, S., Singleton, A., Carrao, H., Vogt, J., 2012. Development of a Combined Drought Indicator to detect agricultural drought in Europe. Natural Hazards and Earth System Sciences 12, 3519–3531.

Sheffield, J., Wood, E.F., 2008. Projected changes in drought occurrence under future global warming from multi-model, multi-scenario, IPCC AR4 simulations. Clim Dyn 31, 79–105. https://doi.org/10.1007/s00382-007-0340-z

Skahill, B., Berenguer, B., Stoll, M., 2021. Ensembles for Viticulture Climate Classifications of the Willamette Valley Wine Region. Climate 9, 140. https://doi.org/10.3390/cli9090140

Svoboda, M., LeComte, D., Hayes, M., Heim, R., Gleason, K., Angel, J., Rippey, B., Tinker, R., Palecki, M., Stooksbury, D., Miskus, D., Stephens, S., 2002. The Drought Monitor. Bulletin of the American Meteorological Society 83, 1181–1190. https://doi.org/10.1175/1520-0477-83.8.1181

Tebaldi, C., Debeire, K., Eyring, V., Fischer, E., Fyfe, J., Friedlingstein, P., Knutti, R., Lowe, J., O'Neill, B., Sanderson, B., van Vuuren, D., Riahi, K., Meinshausen, M., Nicholls, Z., Tokarska, K.B., Hurtt, G., Kriegler, E., Lamarque, J.-F., Meehl, G., Moss, R., Bauer, S.E., Boucher, O., Brovkin, V., Byun, Y.-H., Dix, M., Gualdi, S., Guo, H., John, J.G., Kharin, S., Kim, Y., Koshiro, T., Ma, L., Olivié, D., Panickal, S., Qiao, F., Rong, X., Rosenbloom, N., Schupfner, M., Séférian, R., Sellar, A., Semmler, T., Shi, X., Song, Z., Steger, C., Stouffer, R., Swart, N., Tachiiri, K., Tang, Q., Tatebe, H., Voldoire, A., Volodin, E., Wyser, K., Xin, X., Yang, S., Yu, Y., Ziehn, T., 2021. Climate model projections from the Scenario Model Intercomparison Project (ScenarioMIP) of CMIP6. Earth System Dynamics 12, 253–293. https://doi.org/10.5194/esd-12-253-2021

The Mathworks Inc., 2019. Parallel Computing Toolbox version 9.6.0 (R2019a).

The Mathworks Inc., 2019a. MATLAB version 9.6.0 (R2019a).

The Mathworks Inc., 2019b. Statistics and Machine Learning Toolbox version 9.6.0 (R2019a).

Timbal, B., Jones, D.A., 2008. Future projections of winter rainfall in southeast Australia using a statistical downscaling technique. Climatic Change 86, 165–187. https://doi.org/10.1007/s10584-007-9279-7

Trenberth, K.E., Dai, A., van der Schrier, G., Jones, P.D., Barichivich, J., Briffa, K.R., Sheffield, J., 2014. Global warming and changes in drought. Nature Clim Change 4, 17–22. https://doi.org/10.1038/nclimate2067

Vrac, M., Noël, T., Vautard, R., 2016. Bias correction of precipitation through Singularity Stochastic Removal: Because occurrences matter. Journal of Geophysical Research: Atmospheres 121, 5237–5258. https://doi.org/10.1002/2015JD024511

White, D.H. and Bordas, V. 1997. Proceedings of a workshop on Indicators of Drought Exceptional Circumstances. Bureau of Resource Sciences, Canberra, 1 October 1996, 87 pp.

White, D.H., Karssies, L., 1999. Australia's national drought policy: aims, analyses and implementation. Water International 24, 2–9.

White, D.H., Walcott, J.J., 2009. The role of seasonal indices in monitoring and assessing agricultural and other droughts: a review. Crop Pasture Sci. 60, 599–616. https://doi.org/10.1071/CP08378

Wilhite, D.A., Sivakumar, M.V., Pulwarty, R., 2014. Managing drought risk in a changing climate: The role of national drought policy. Weather and climate extremes 3, 4–13.

Wittwer, G., Waschik, R., 2021. Estimating the economic impacts of the 2017–2019 drought and 2019–2020 bushfires on regional NSW and the rest of Australia. Australian Journal of Agricultural and Resource Economics 65, 918–936. https://doi.org/10.1111/1467-8489.12441

Xu, C.-Y., Singh, V., 2002. Cross comparison of empirical equations for calculating potential evapotranspiration with data from Switzerland. Water Resources Management 16, 197–219.

Yan, Z., Bate, S., Chandler, R.E., Isham, V., Wheater, H., 2002. An Analysis of Daily Maximum Wind Speed in Northwestern Europe Using Generalized Linear Models. Journal of Climate 15, 2073–2088. https://doi.org/10.1175/1520-0442(2002)015<2073:AAODMW>2.0.CO2